BREAK-OUT SESSION 4

SUBORBIT & BIOMASS

TSIGARIDIS (MODERTAOR) / **HICKMAN** (RAPPORTEUR)

Ferrare, Richard	**Biomass Burning over the SE Atlantic**
Eck, Thomas	**AERONET ext. wavelength retrievals of absorption**
Puthukkudy, Anin	**Aerosol properties from the AirHARP Polarimeter**
Johnson, Ben	**Self-raising aerosol**
Bellouin, Nicolas	Impact of Chinese Covid-19 lockdown
Kondragunta, Shobha	China and Taiwan: 2 diff COVID-19 lockdowns
Liu, Xiaohong	Impacts of COVID-19 on rad. forcing
Mortier, Augustin	COVID-19: Impact on AOD and EU Air Quality
Quaas, Johannes	Aviation-induced cirrus during COVID-19
Skeie, Ragnhild	Aerosol and rad. forcing due to COVID-19
Tsyro, Svetlana	Impacts of COVID-19 lockdown on EU air quality

Analysis of AERONET Extended Wavelength Retrievals of Aerosol Absorption Parameters Including 380 nm and 500 nm for Detection of Brown Carbon in Biomass Burning and Iron Oxides in Desert Dust

Thomas F. Eck[1,2], Brent N. Holben[2], Alexander Sinyuk[3,2], David M. Giles[3,2], Ilya Slutsker[3,2], Joel S. Schafer[3,2], Mikhail G. Sorokin[3,2], Alexander Smirnov[3,2], Anthony D. LaRosa[3,2], Jason Kraft[4,2]
(1) Universities Space Research Association, Columbia, MD, USA; (2) NASA/GSFC, Greenbelt, MD, USA; (3) Science Systems Applications, Inc., Lanham, MD, USA; (4) Fibertek Inc., Herndon, VA, USA

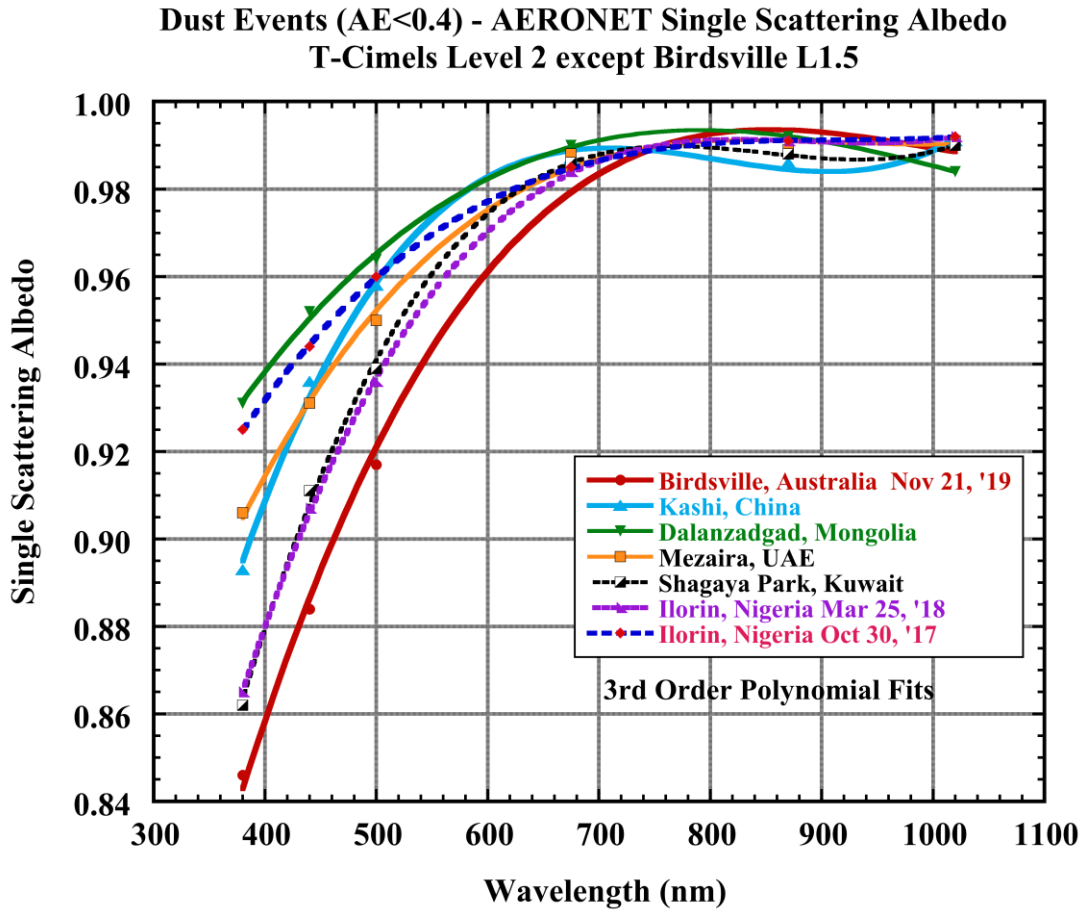

Comparison of spectral SSA from AERONET retrievals (AE<0.4) from various dust sources and/or regions: Most weakly absorbing dust at 380 nm from Ilorin with trajectory from the Bodele, also a case from Mongolia. Strongest absorption from Australia (red soils with high iron oxides). Similar SSA at all sites for λ >600 nm.

Comparison of AERONET retrievals to in situ Lab measurements

Atmos. Chem. Phys., 19, 15503–15531, 2019
https://doi.org/10.5194/acp-19-15503-2019
© Author(s) 2019. This work is distributed under the Creative Commons Attribution 4.0 License.

Atmospheric Chemistry and Physics

Complex refractive indices and single-scattering albedo of global dust aerosols in the shortwave spectrum and relationship to size and iron content

Claudia Di Biagio[1], Paola Formenti[1], Yves Balkanski[2], Lorenzo Caponi[1,3], Mathieu Cazaunau[1], Edouard Pangui[1], Emilie Journet[1], Sophie Nowak[1], Meinrat O. Andreae[1,4], Konrad Kandler[5], Thuraya Saeed[6], Stuart Piketh[6], David Seibert[1,6], Earle Williams[1,7], and Jean-François Doussin[1]

Table 5. As in Table 4 for the single-scattering albedo (SSA) data. Mean, m

Sample region	SSA						
	0.37 µm	0.47 µm	0.52 µm	0.59 µm	0.66 µm	0.88 µm	0.95 µm
Tunisia	0.85	0.90	0.93	0.95	0.95	0.97	0.97
Morocco	0.92	0.95	0.96	0.98	0.98	0.98	0.99
Libya	0.89	0.93	0.95	0.98	0.98	0.98	0.98
Algeria	0.87	0.92	0.94	0.97	0.97	0.98	0.98
Mauritania	0.85	0.90	0.94	0.96	0.97	0.98	0.98
NAF–S	**0.88**	**0.92**	**0.94**	**0.97**	**0.97**	**0.98**	**0.98**
Niger	0.72	0.85	0.89	0.91	0.92	0.94	0.95
Mali	0.75	0.85	0.89	0.93	0.95	0.96	0.96
Bodélé	0.96	0.98	0.98	0.99	0.99	0.99	0.99
SAH	**0.81**	**0.89**	**0.92**	**0.94**	**0.95**	**0.96**	**0.97**
Ethiopia	0.80	0.86	0.90	0.92	0.94	0.97	0.97
Saudi Arabia	0.88	0.93	0.96	0.98	0.98	0.98	0.98
Kuwait	0.95	0.97	0.98	0.98	0.99	0.99	0.99
EAF–ME	**0.88**	**0.92**	**0.94**	**0.96**	**0.97**	**0.98**	**0.98**
Gobi	0.88	0.92	0.94	0.96	0.97	0.97	0.97
Taklimakan	0.82	0.88	0.92	0.95	0.96	0.96	0.96
EA	**0.85**	**0.90**	**0.93**	**0.96**	**0.96**	**0.97**	**0.97**
Arizona	0.93	0.96	0.97	0.98	0.98	0.99	0.99
NAM	**0.93**	**0.96**	**0.97**	**0.98**	**0.98**	**0.99**	**0.99**
Atacama	0.89	0.93	0.94	0.97	0.97	0.98	0.98
Patagonia	0.88	0.91	0.94	0.96	0.97	0.98	0.98
SAM	**0.89**	**0.92**	**0.94**	**0.96**	**0.97**	**0.98**	**0.98**
Namib-1	0.91	0.95	0.96	0.98	0.98	0.99	0.99
Namib-2	0.74	0.82	0.86	0.92	0.94	0.96	0.97
SAF	**0.83**	**0.88**	**0.91**	**0.95**	**0.96**	**0.98**	**0.98**
Australia	0.70	0.81	0.85	0.91	0.93	0.96	0.97
AUS	**0.70**	**0.81**	**0.85**	**0.91**	**0.93**	**0.96**	**0.97**
Mean	**0.85**	**0.91**	**0.93**	**0.96**	**0.96**	**0.97**	**0.98**
Median	**0.88**	**0.92**	**0.94**	**0.96**	**0.97**	**0.98**	**0.98**
10 %	**0.74**	**0.84**	**0.88**	**0.92**	**0.94**	**0.96**	**0.96**
90 %	**0.93**	**0.96**	**0.97**	**0.98**	**0.99**	**0.99**	**0.99**

Di Biagio et al. (2019) measured spectral absorption in a laboratory from soil samples collected from around the world. Soil dust was suspended in a smog chamber for measurements of scattering and absorption coeff. to be made. The least absorbing dust came from samples taken in the Bodele, with SSA at 370 nm of 0.96, while the most absorbing sample came from Australia with SSA at 370 nm of 0.70. From the AERONET cases shown in the plot at left the most absorbing is from Birdsville, Australia with SSA at 380 nm ~0.84, while the least absorbing is from Mongolia and Ilorin, Nigeria ~0.93. For the weakly absorbing case in Nigeria the back trajectory suggests some origin from over the Bodele Depression. Therefore we see general agreement in the dust source regions for strongly and weakly absorbing particles, although the extremes are much greater in the lab data of Di Biagio et al. (2019). This may be due in part to dust from several sources mixing together in the transported aerosol plumes measured by AERONET.

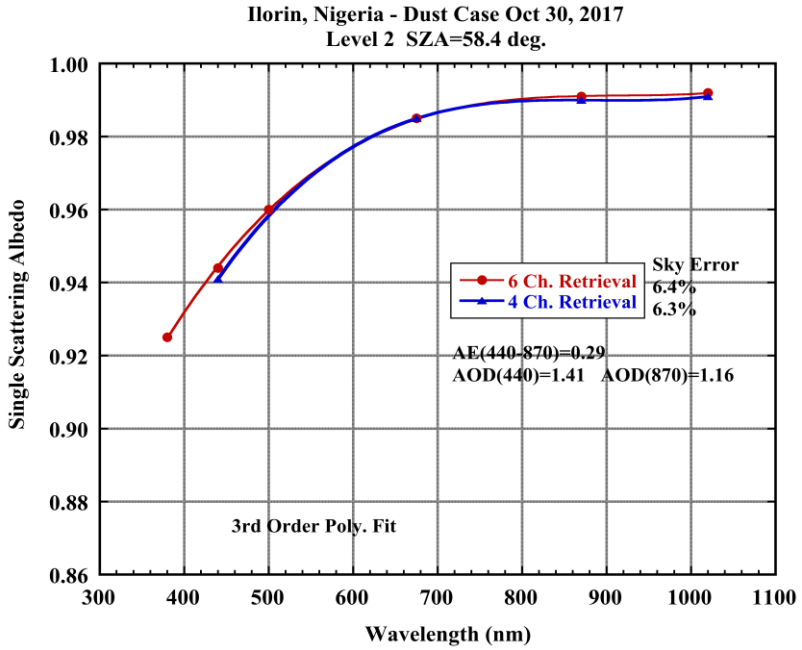

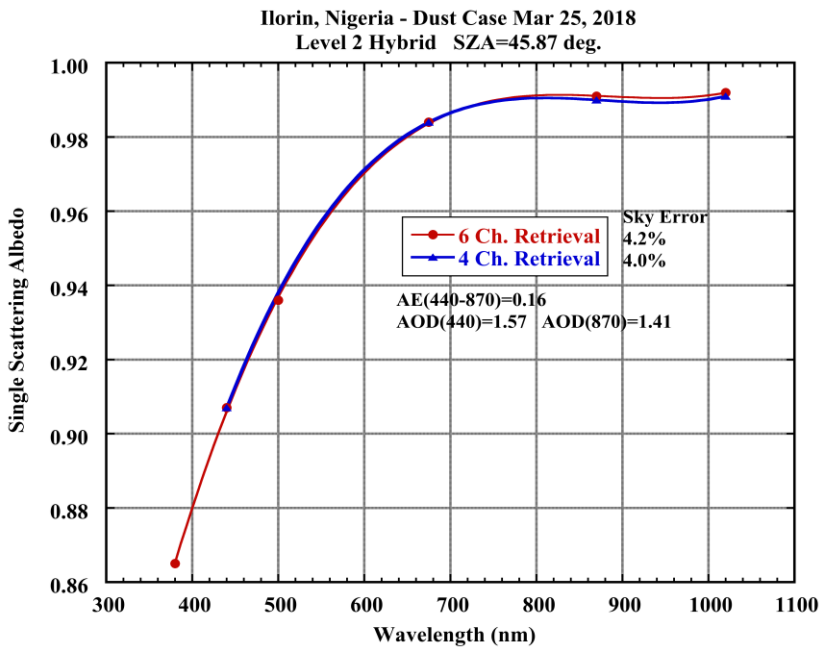

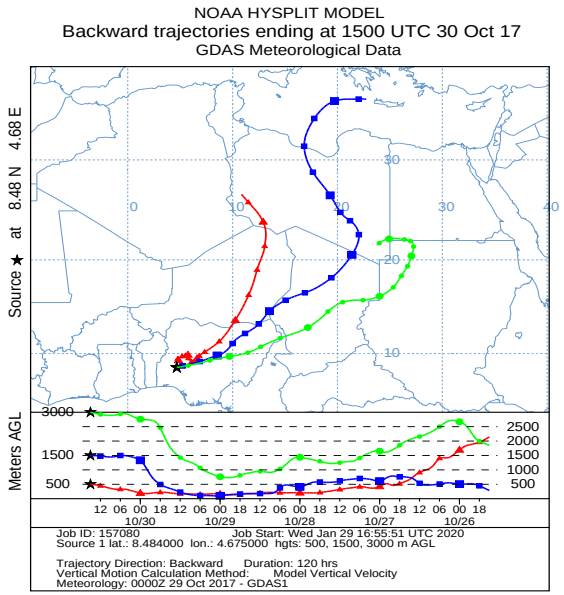

Oct. 30, 2017 trajectory in blue passes directly over the Bodele Depression which is a source of very weakly absorbing diatomite sediments. Mar 25, 2028 trajectory in blue passes over a different region of the Sahara, not even close to the Bodele Depression.

The higher SSA in the Oct 30, 2017 retrievals is consistent with the characteristics of the mineral source in the Bodele Depression

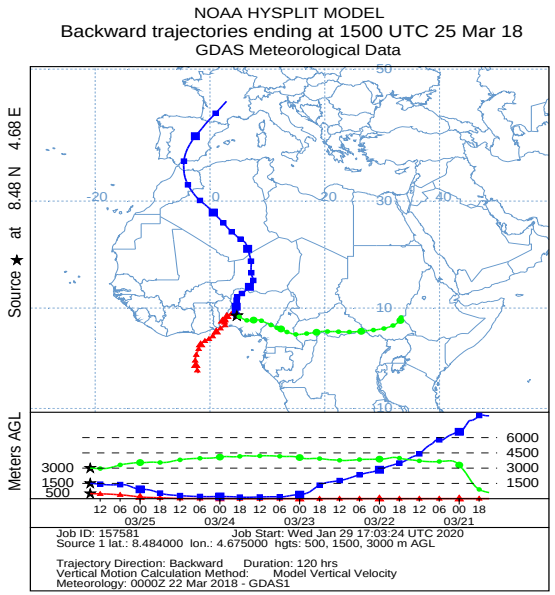

Ilorin, Nigeria AERONET site

Significant differences in dust absorption on different dates of large dust events (AOD(440)>1.4 for both).

Back trajectories suggest that dust in these events originated from different source regions

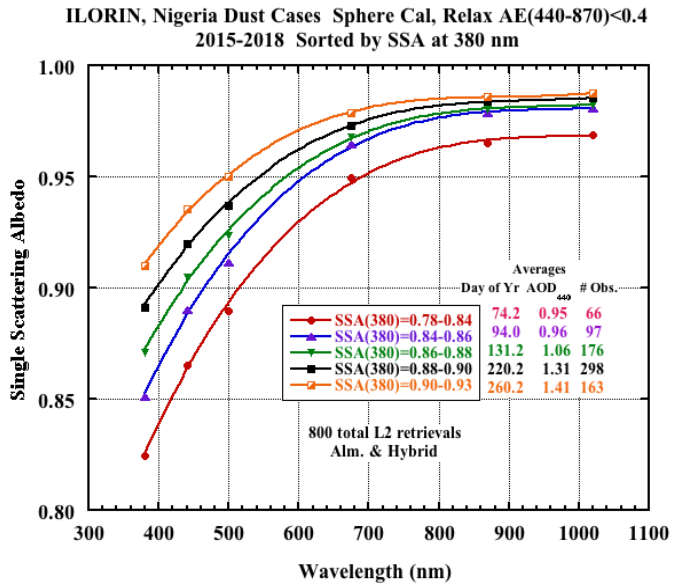

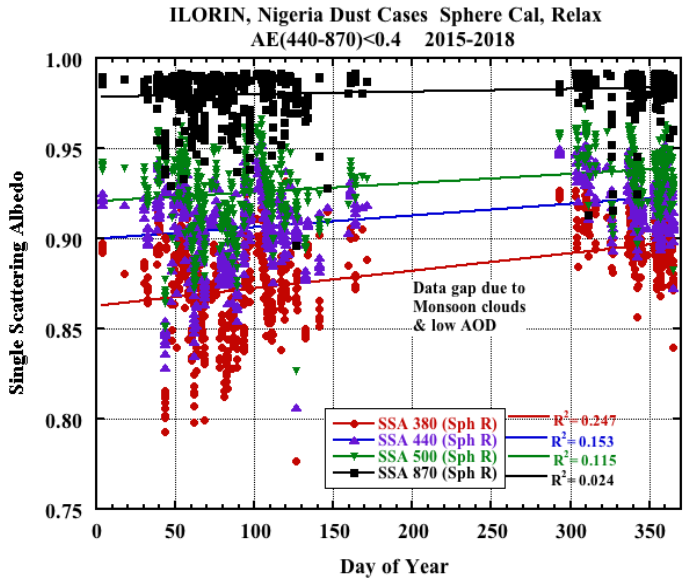

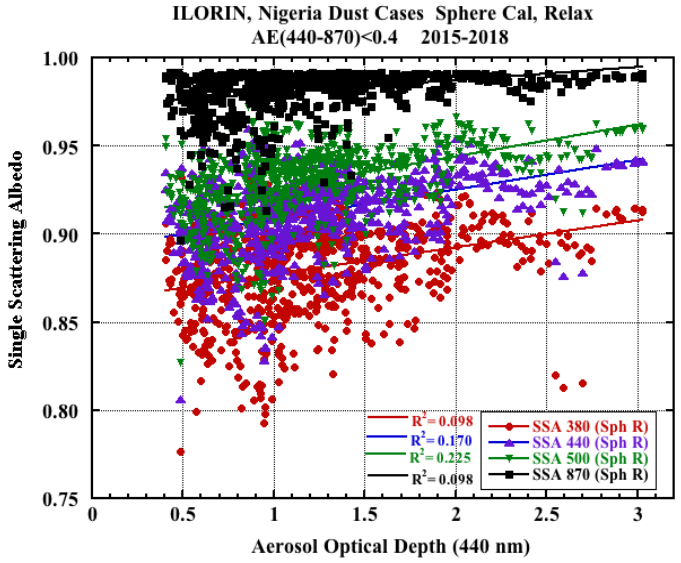

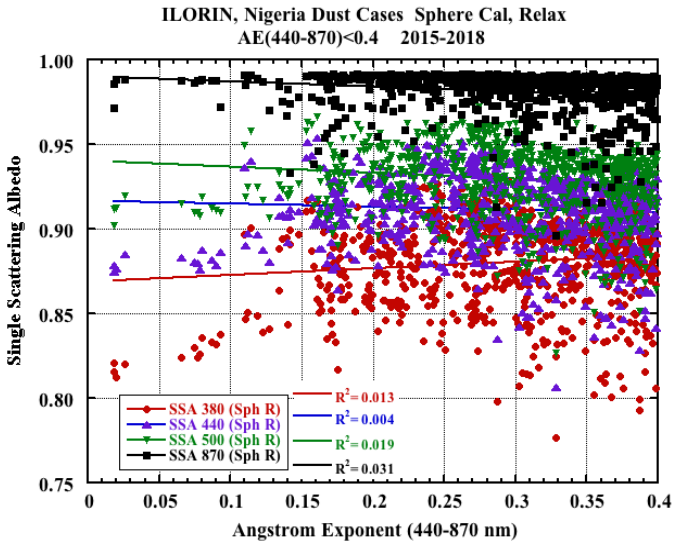

Ilorin, Nigeria:

SSA from Feb-May is lower at shorter wavelengths than from October - December, possibly due to more transport from the Bodele to Ilorin in the fall season.

SSA increases as AOD increases, possibly in part due to the Bodele Depression events having both very high AOD and very low SSA (weak absorption in diatomaceous sediment versus iron oxides in mineral dust)

The data gap in January is likely due to lack of AE<0.4 due to biomass burning smoke mixing with dust

Kanpur, India: Strong trend of decreasing absorption through the spring to fall seasons at all wavelengths, greatest at shortest wavelengths (possible BC coating on dust - note that longer λ SSA increases also); no trend as a function of AOD; trend as a function of AE is only significant at longer wavelengths (r^2=0.25 at 870 nm)

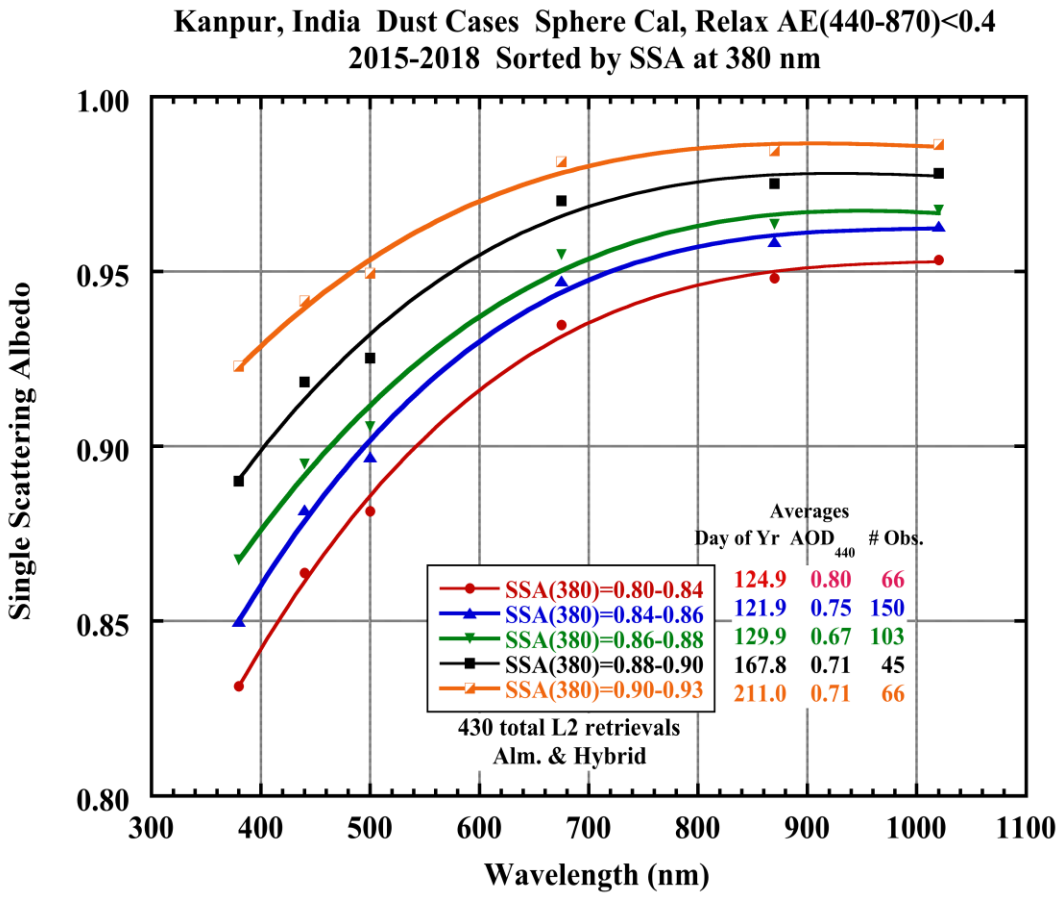

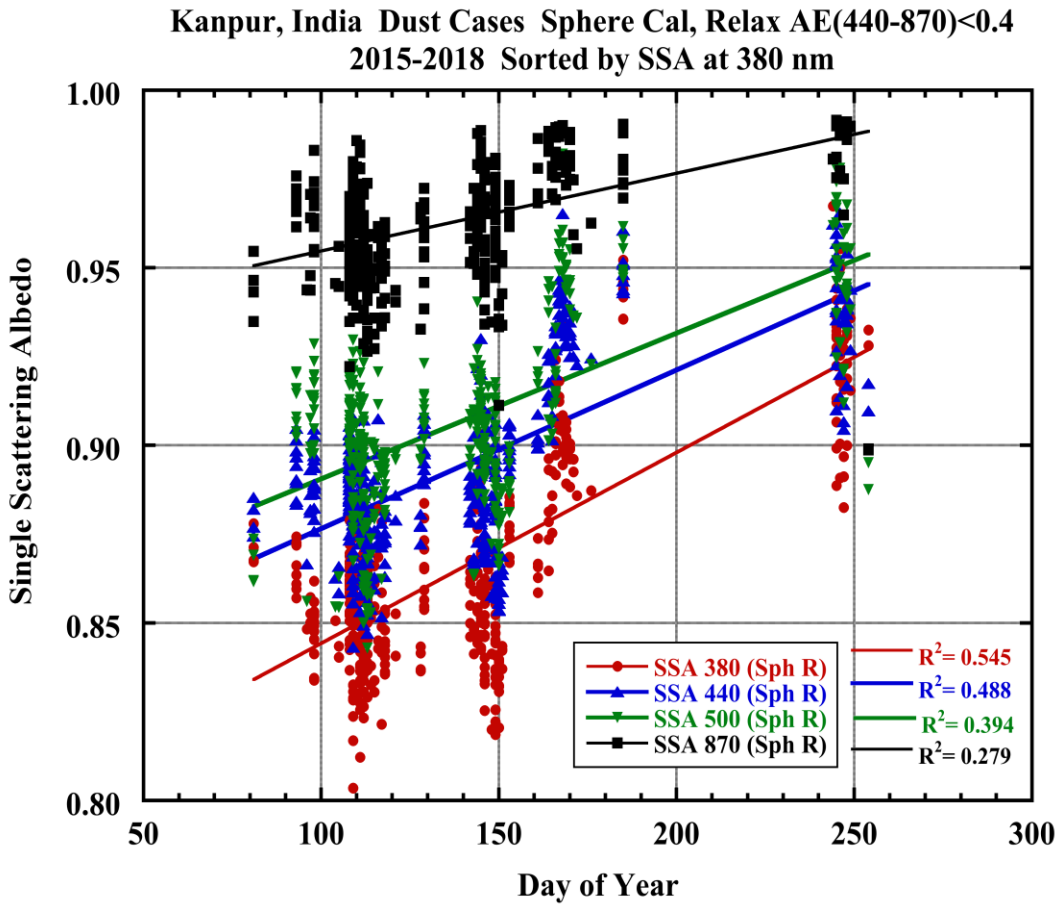

GSFC Sep 15, ’20: Long distance smoke transport from California

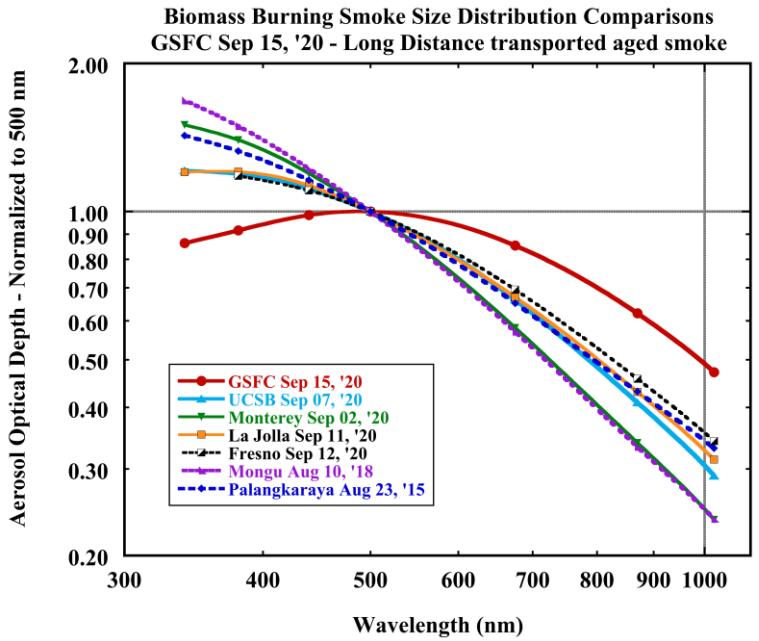

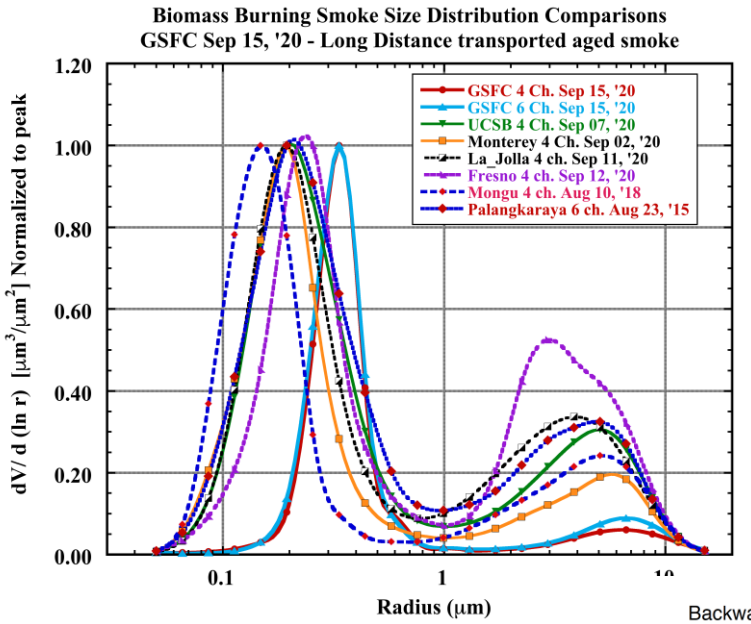

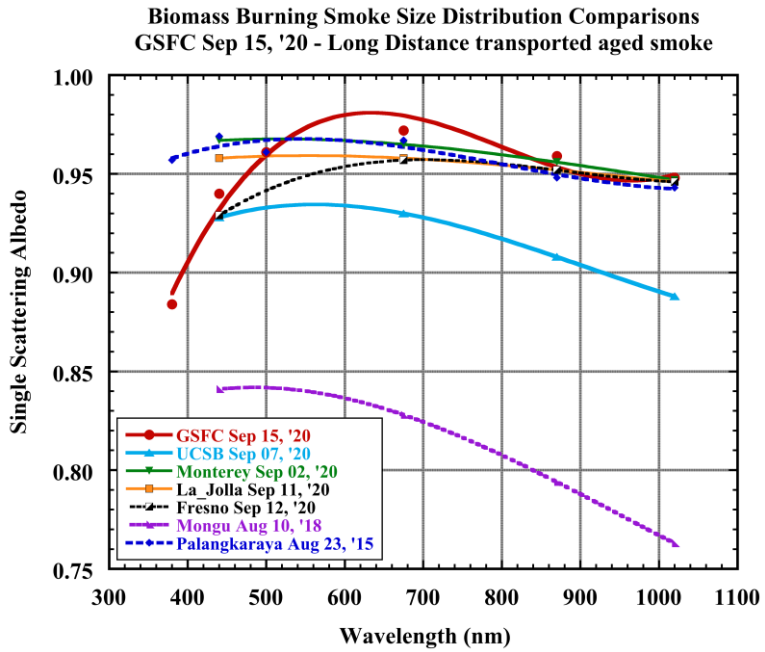

- **Normalized (to 500nm) AOD spectra at GSFC show extremely unusual decreases <500 nm.** At the La Jolla, UCSB and Fresno cases the AOD spectra show at flattening from 380 to 340 nm, when this smoke was close to the fire sources.
- **Normalized size distributions (to peak concentration values) comparisons to the GSFC case on Sep 15, ‘20 shows fine mode is significantly larger in radius and also much narrower in width**
- **Spectral SSA at GSFC for the Sep 15, ‘20 case shows strong absorption at 380 nm relative to 500 nm suggesting significant Brown Carbon absorption,** but also due to decreased scattering optical depth <500 nm due to the large size with narrow width fine mode size distribution
- AOD computed from the retrieved size distribution and refractive indices for the GSFC case matches the measured AOD to within 0.001 at all channels.

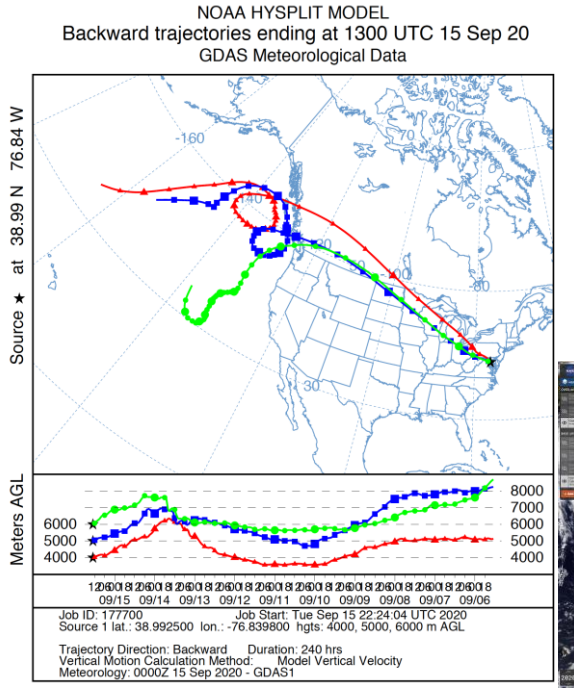

HYSPLIT Back-Trajectory shows that the air that arrived at GSFC at 6 km on Sep 15 was located over the Pacific off the west coast of California and Oregon from Sep 8 through Sep 12, 2020. MPL backscatter at GSFC showed aerosol layer at 4-6 km altitude on Sep 15. This smoke is aging for a few days in an elevated layer over the Pacific Ocean, with some input from active fires each day, until it is advected towards the East coast (Sep 10 Aqua image below)

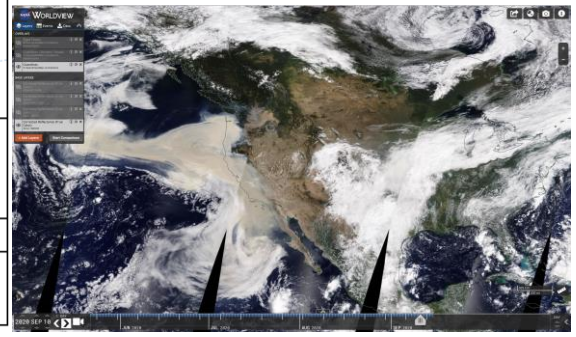

Background: V4 Operational CALIOP Measurements of Smoke above Clouds Over Southeast Atlantic Ocean Can Be Problematic

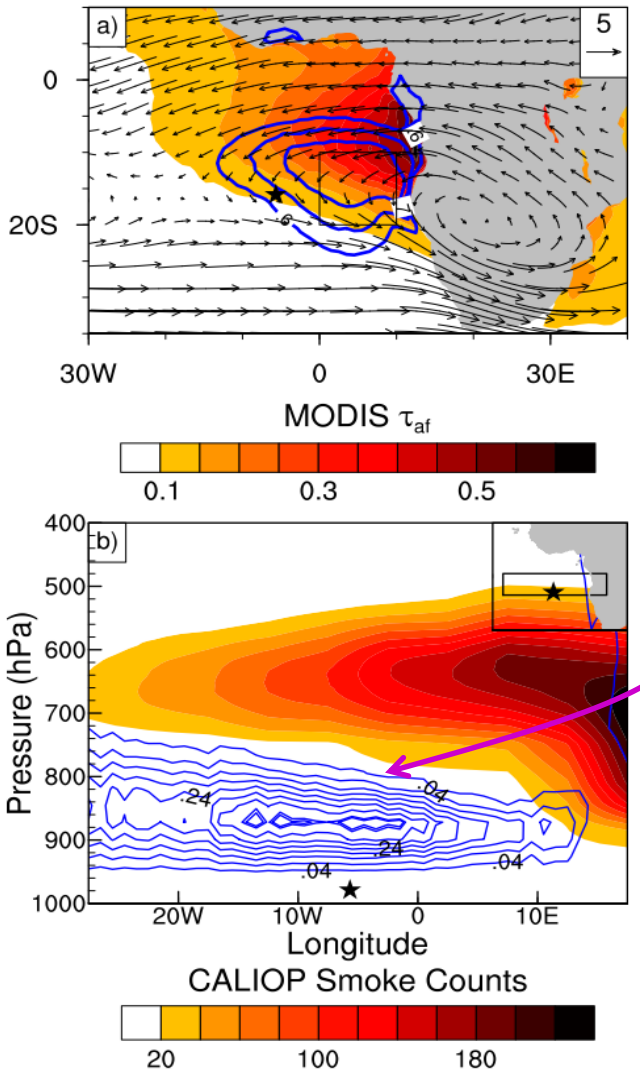

e.g. Adebiyi et al., 2015

- Proximity of smoke to clouds impacts cloud drop size, cloud coverage, etc. and consequently cloud radiative impacts
- CALIOP aerosol profiles have been used to determine proximity of elevated smoke layers to underlying clouds
- Problem: CALIOP V4 532 nm aerosol layer detection often misses lower boundary of thick smoke layer due to strong attenuation of upper part of smoke layer (current V4 algorithm CALIOP 1064 nm penetrates further but uses 532 nm layer boundaries) resulting in:
  - Underestimate of above cloud AOD (ACAOD)
  - Overestimate in the size of the gap between smoke and cloud

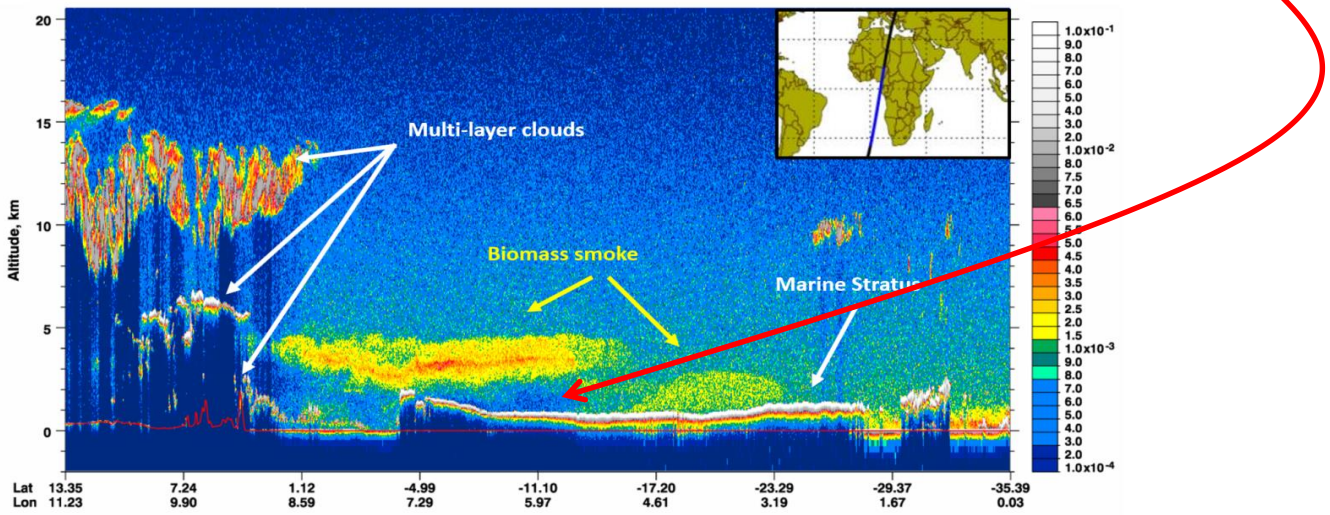

Solution: Opaque Water Cloud ("Depolarization Ratio Method") Provides Alternative (and Better) Method to Derive Above Cloud AOD (ACAOD) and Aerosol Extinction Profiles

1. V4 Operational product uses
   - layer detection scheme
   - extinction retrieval algorithm
   - inferred lidar ratio
2. Opaque water cloud ("Depolarization Ratio" – Hu et al., 2007; Deaconu et al., 2017)) uses
   - Layer-integrated attenuated backscatter and depolarization of clouds
   - Assumed cloud lidar ratio (18.9 sr)

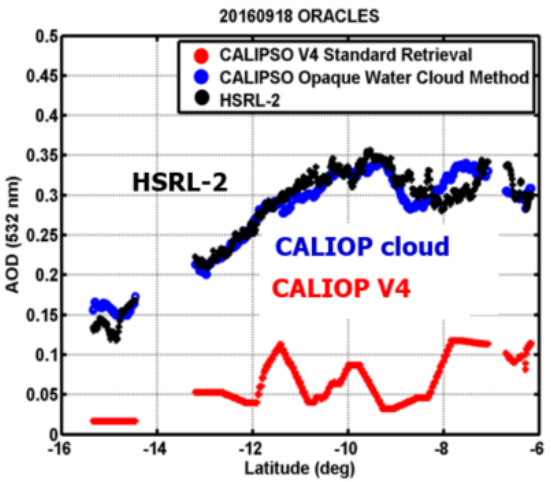

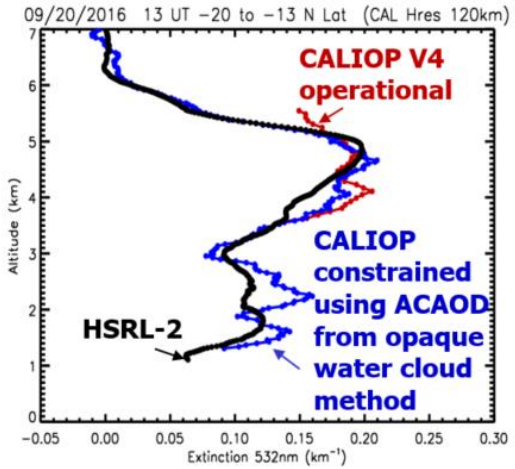

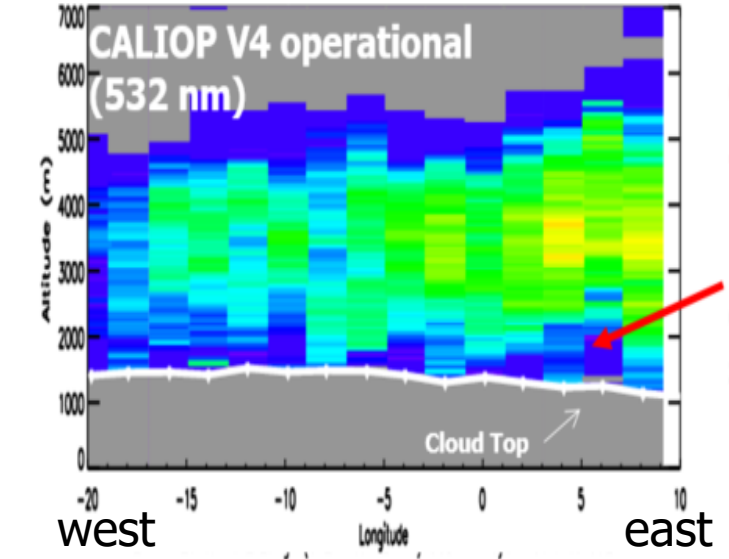

CALIOP V4 operational algorithm (532 nm).

Note the gap between the cloud top and the bulk of the smoke layer.

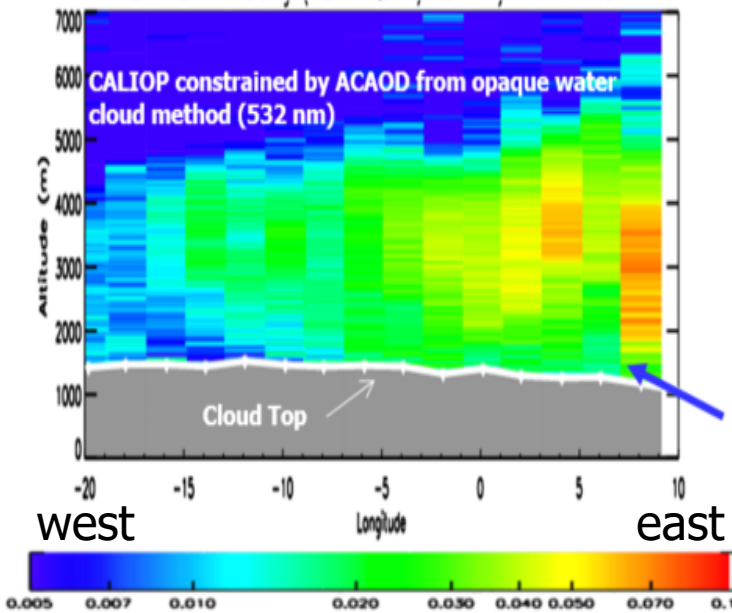

Profiles derived using the ACAOD constraint obtained from the CALIOP opaque water cloud ("Depolarization Ratio – DR") method.

Gap has significantly reduced so that smoke and clouds are in close proximity most of the time.

Averaged ACAOD (532 nm), Aerosol Angström exponent (532-1064 nm), and Lidar Ratio computed using CALIOP ACAOD constraint (2006-2018)

- CALIOP profiles (2006-2018), constrained by the CALIOP above cloud AOD derived using the return signals from the underlying clouds, show that moving west (away) from the African coast and from August to October:
  - Aerosol optical thickness decreases
  - Aerosol Angstrom exponent decreases (~ aerosol size increases)
  - Lidar ratio decreases (~ aerosol absorption decreases)
- Lidar ratio monthly trend is consistent with:
  - HSRL-2 profiles of lidar ratio
  - Decrease in aerosol absorption (increase in SSA) derived from AERONET and OMI (Eck et al., 2013, JGR)

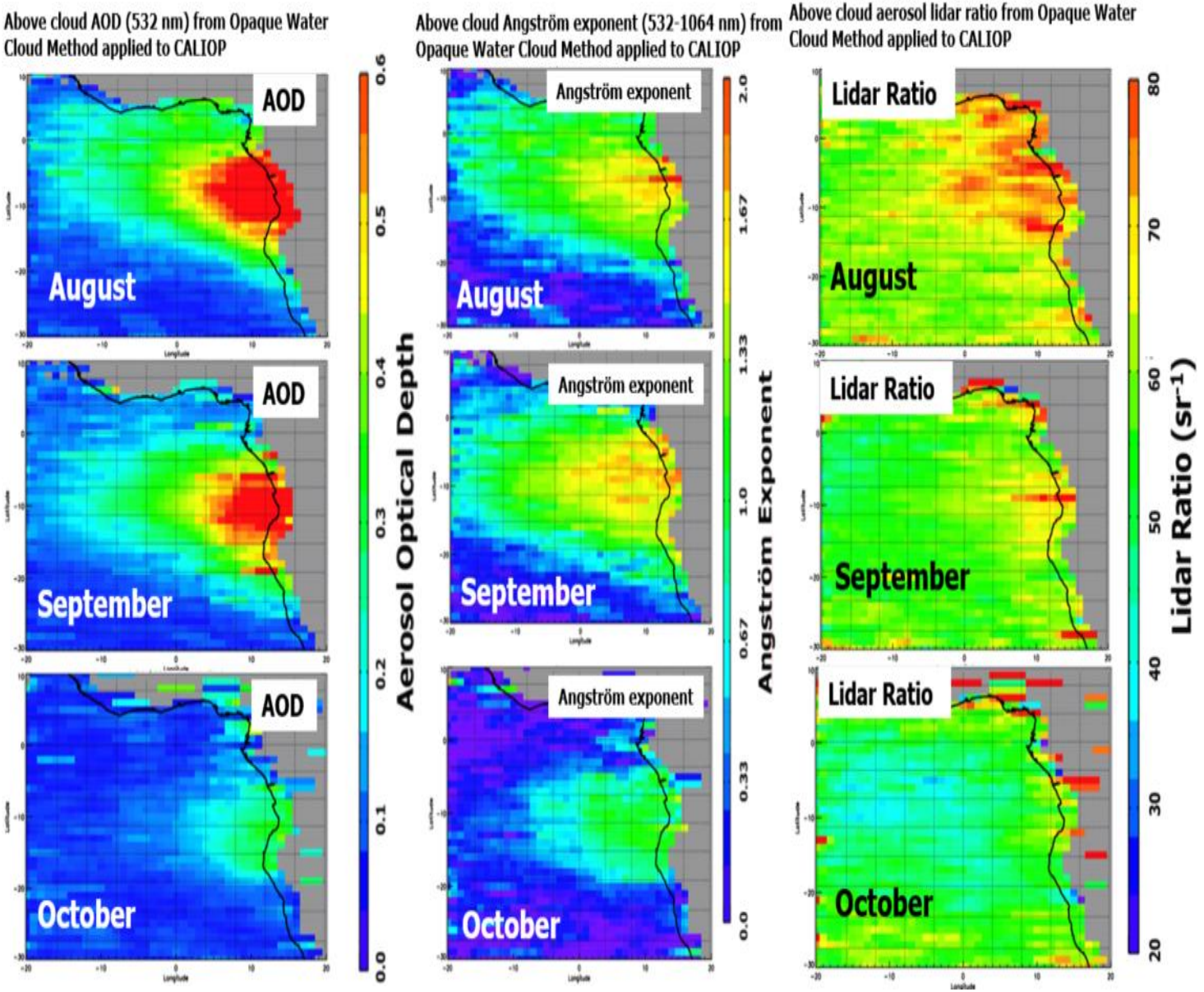

How large is the gap between clouds and smoke layers? (It depends…)

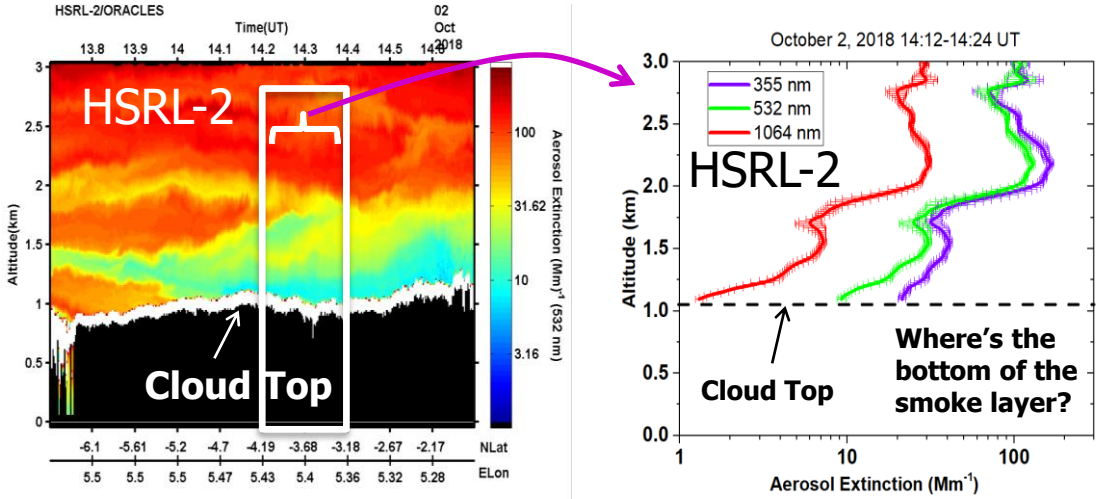

Q. Where's the bottom of the smoke layer?
A. It depends on threshold used to define the bottom.

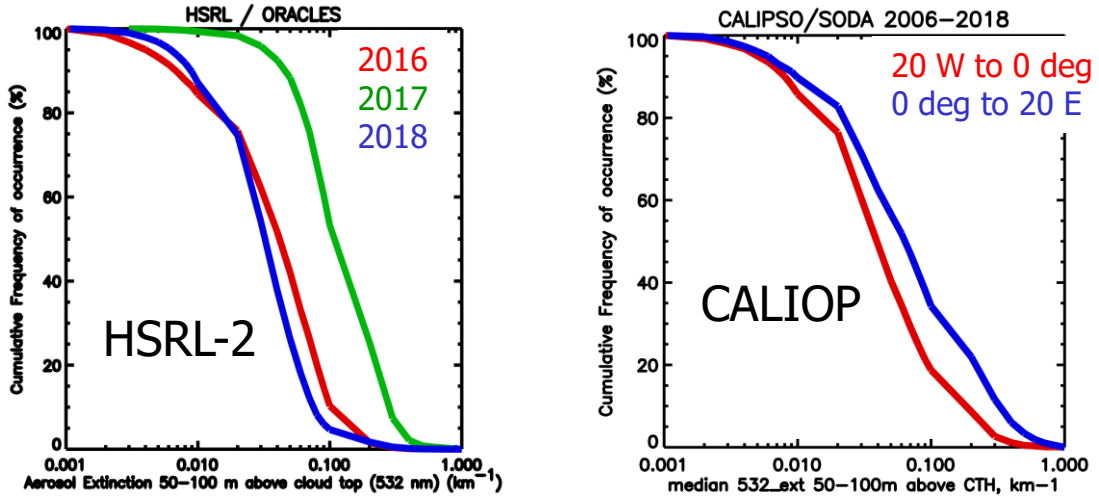

HSRL-2 and CALIOP data show similar distributions of aerosol extinction in the 50-100 m layer above cloud top

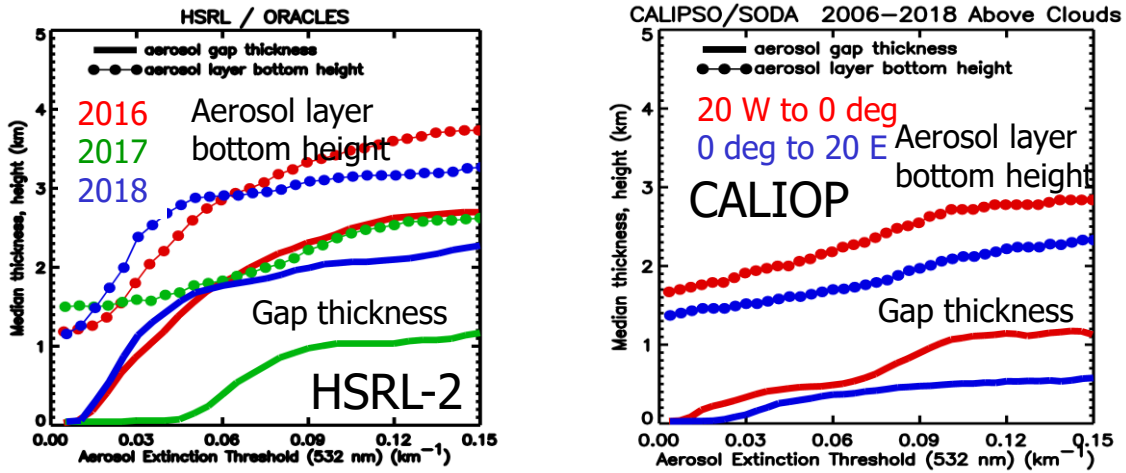

HSRL-2 and CALIOP data show how aerosol layer bottom and gap thickness depend on aerosol extinction threshold value

HSRL-2 data show no correlation between above cloud AOD and aerosol extinction just above cloud top

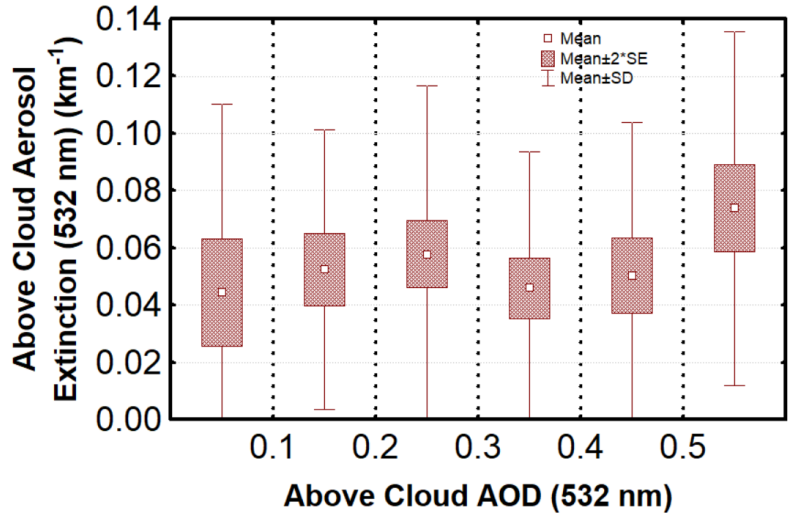

Airborne HSRL-2 Measurements and Retrievals from NASA ORACLES Mission Show Vertical Variability in Median Aerosol Parameters

Airborne HSRL-2 lidar deployed from NASA ER-2 (2016) and P-3 (2017, 2018)

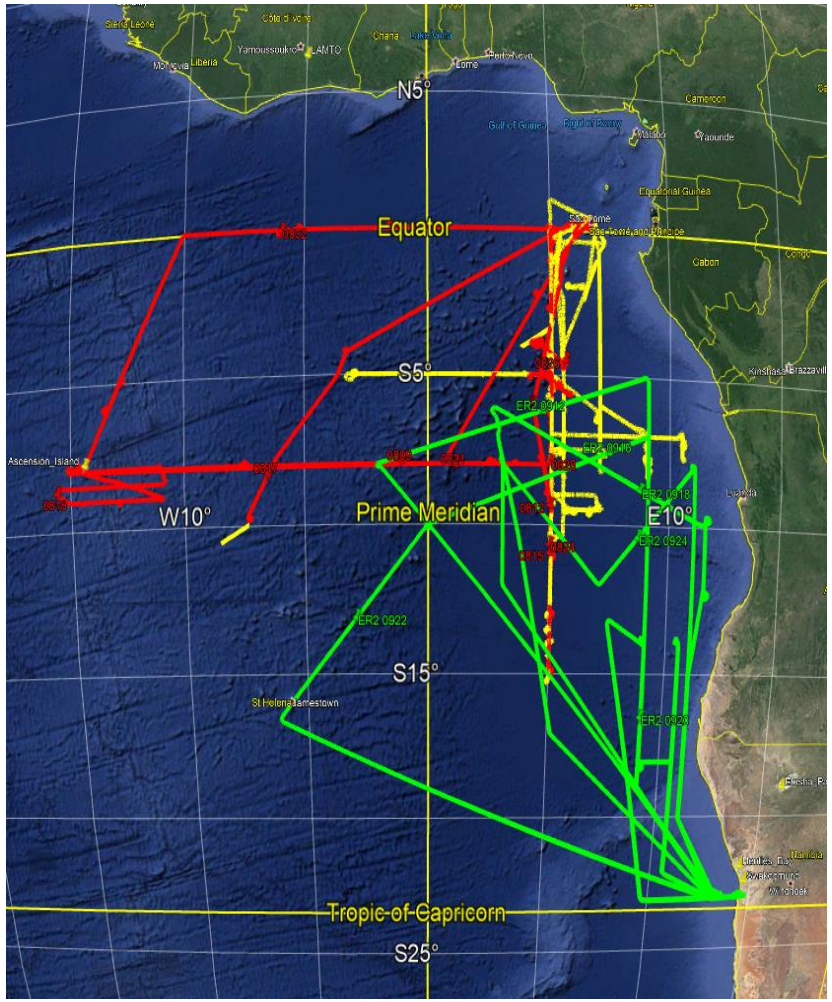

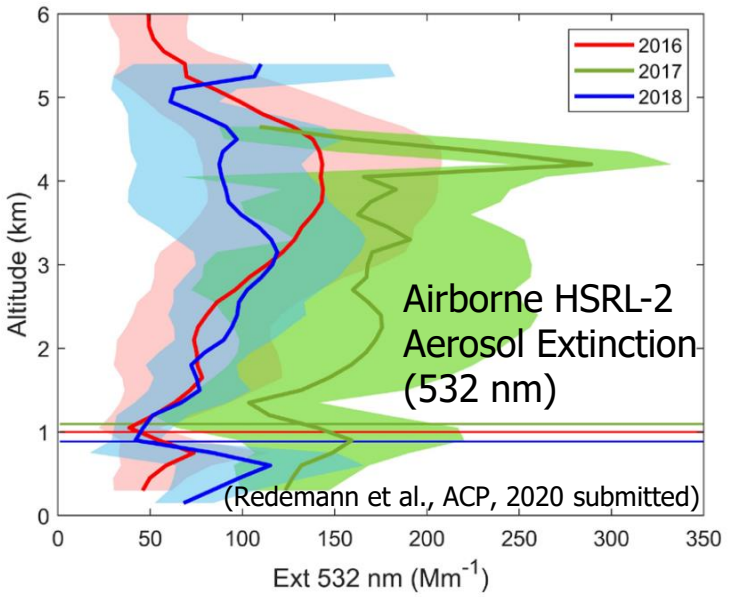

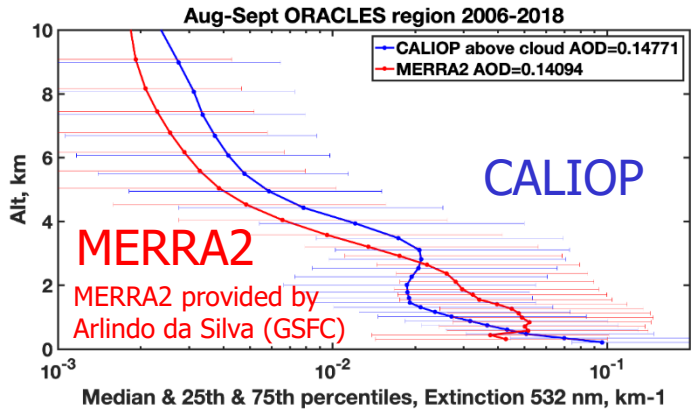

Median CALIOP aerosol extinction profile (2006-2018) shows more aerosol near surface and aloft than MERRA-2 model

Airborne HSRL-2

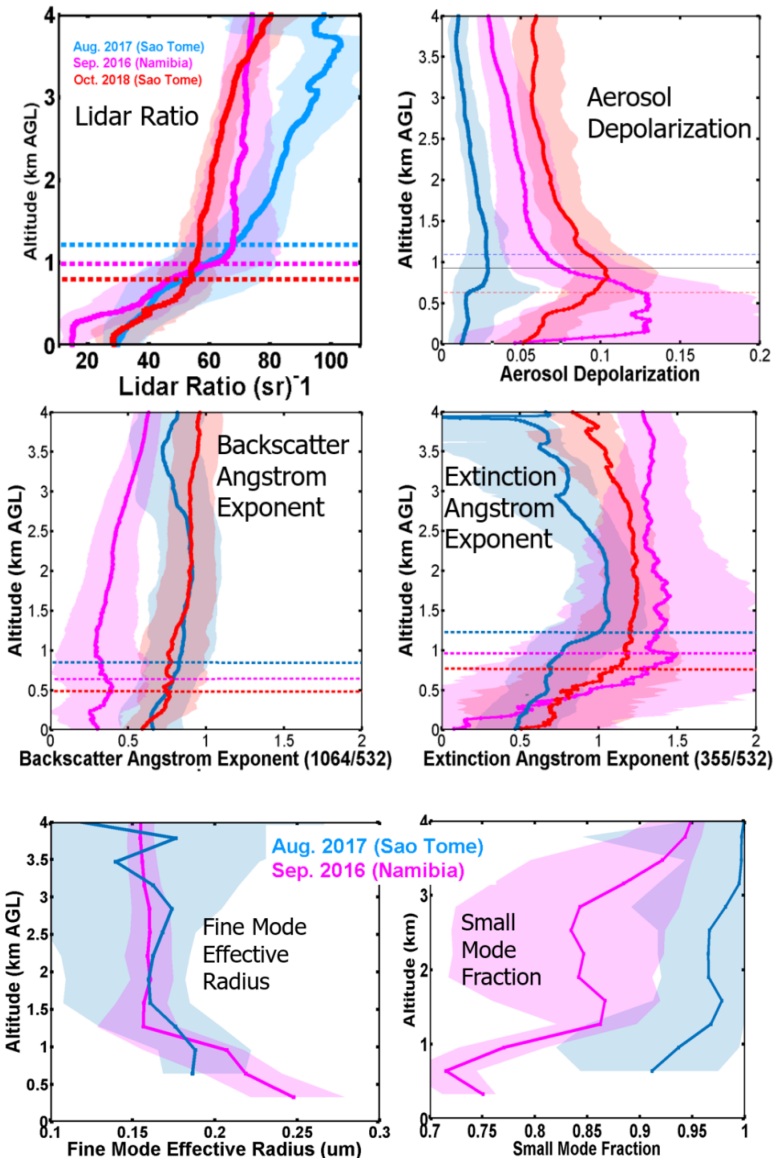

Met Office
Hadley Centre

Self-raising aerosols

Ben Johnson, Jim Haywood

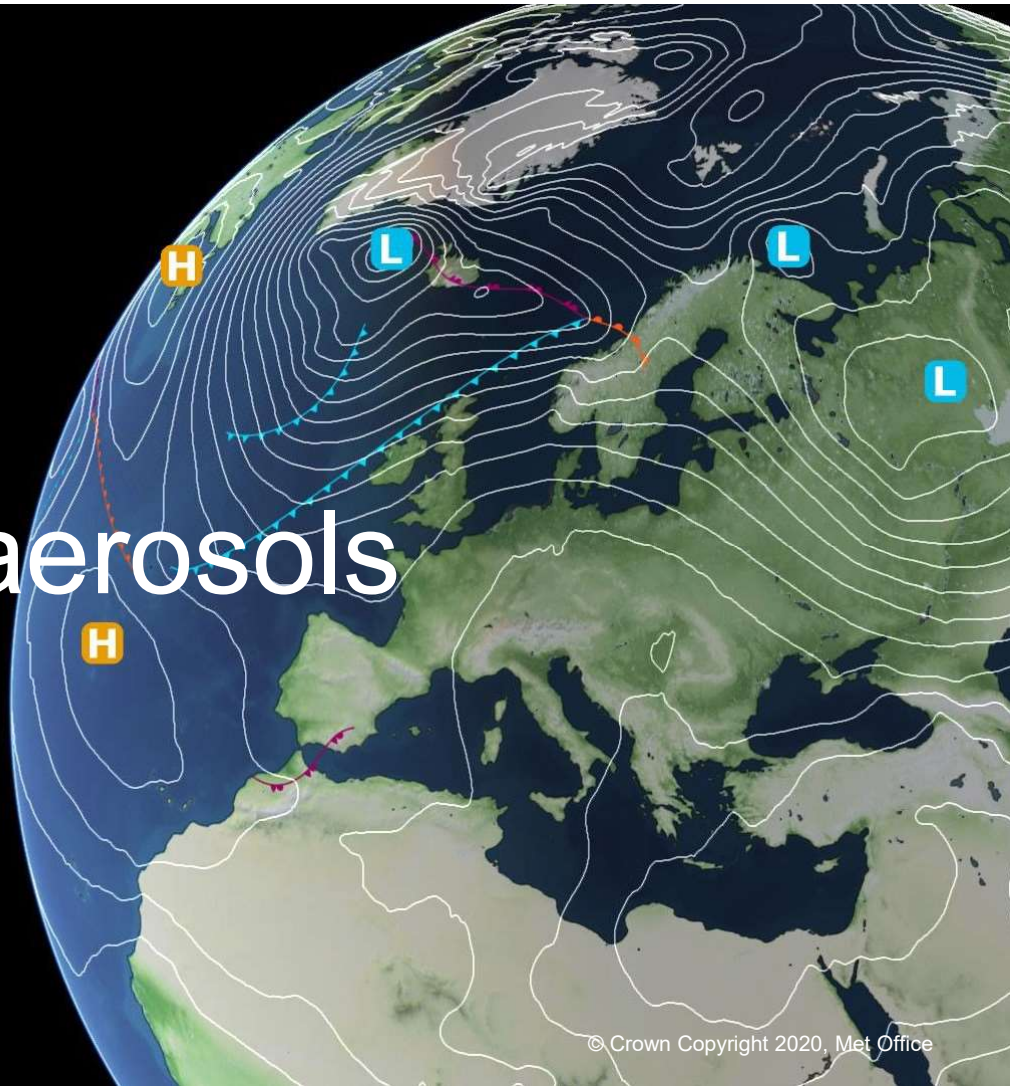

© Crown Copyright 2020, Met Office

Met Office Hadley Centre

Background

- Vertical distribution of aerosol important direct radiative effects, aerosol-cloud interactions, and long-range transport
- Model biases in elevation of absorbing aerosols
- What lifts aerosol vertically?

- Initial buoyancy of plumes from large fires / chimneys
- BL mixing
- Deep convection
- Large-scale ascent
- Numerical diffusion
- Anything else?

Black carbon aerosol is unique as it strongly absorbs solar radiation

- Strong regional impacts on radiative energy balance and precipitation, but these are quite sensitive to altitude of the BC

- Absorb of solar radiation by the BC could help to maintain its buoyancy…

- Does this maintain the buoyancy of the plume or even enhance regional-scale ascent in polluted regions?

BC effective radiative forcing

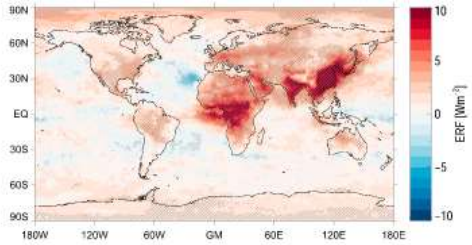

BC induced precipitation change

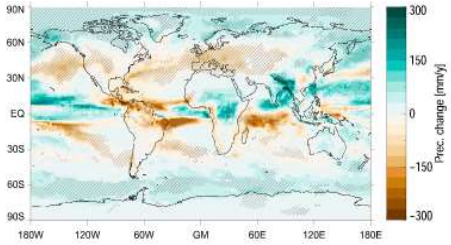

Met Office Hadley Centre

Hypothesis

Radiative heating from BC aerosol elevates aerosols higher in the atmosphere

Experiment with HadGEM3-GA7.1

- **Control simulation** - No BC absorption
- **Experiment** - BC absorption included

- 20 year runs with HadGEM3-GA7.1 (N96)
- Interactive aerosol radiation, cloud and atmos dynamics
- Emissions and SSTs based on 2014 CMI6 timeslice

Global distribution of BC in the atmosphere

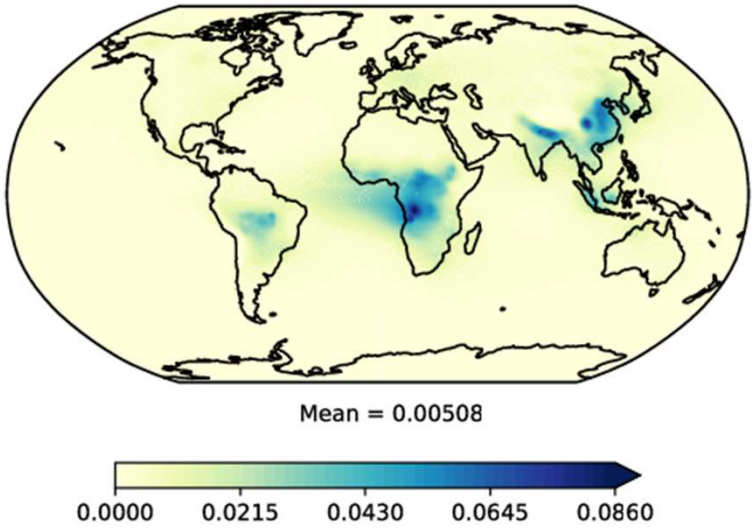

- The abundance of BC aerosol is indicated here by absorption optical depth (AAOD)
- This corresponding to the amount of sunlight the BC can potentially absorb in the atmosphere.
- The radiative heating rate also depends on solar illumination

BC radiative heating in the atmosphere

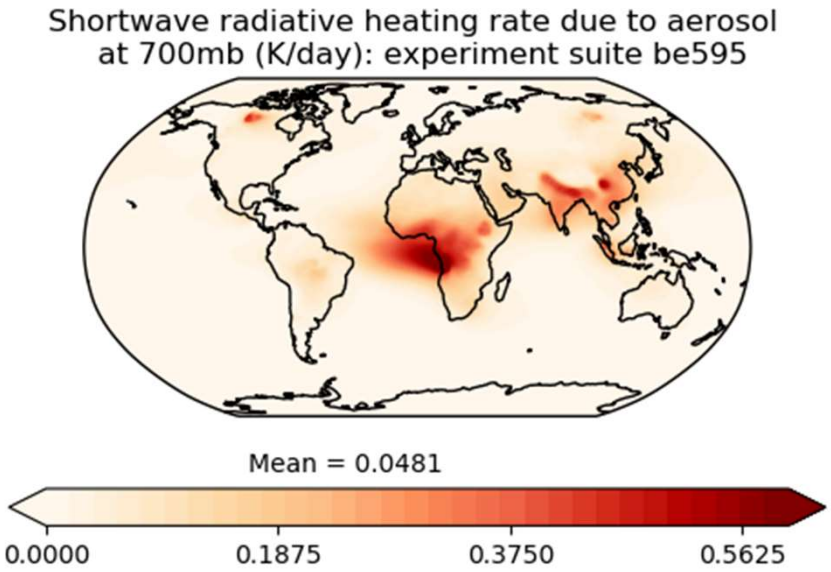

- Plot shows the annual mean from the control simulation
- BC contributed ~90% of the heating
- Remainder was from mineral dust
- Strongest heating at 700mb is from African biomass burning plumes and BC-rich haze over Southern & Eastern Asia

Impact of aerosol absorption on large-scale vertical velocity

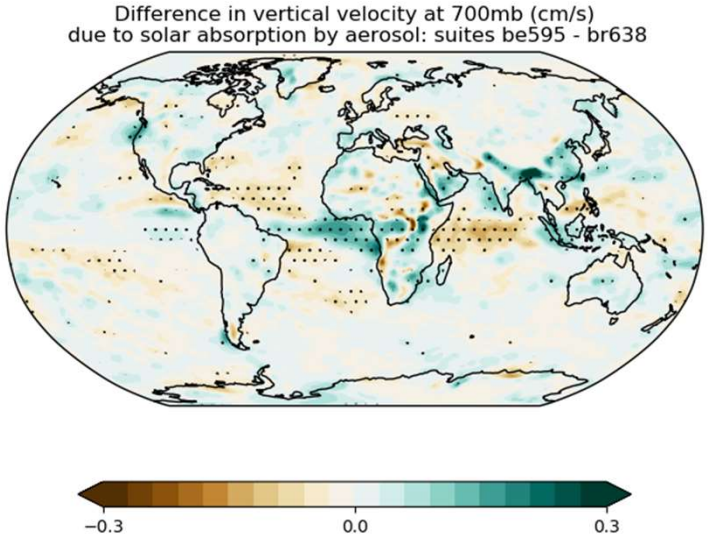

- Statistically significant changes in large-scale vertical motion over broad areas (stipples indicate 95% confidence)
- BC heating causes ascent of around 0.2 cm/s (~ 1km in 5 days) in absorbing aerosol layers over tropical Atlantic and Asia
- Compensating descent in Indian ocean and subtropical Atlantic

Change in BC mass concentration at 600mb

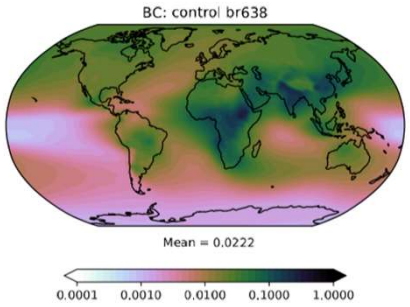

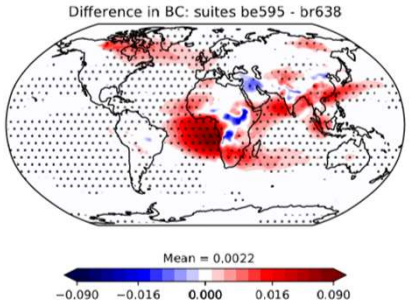

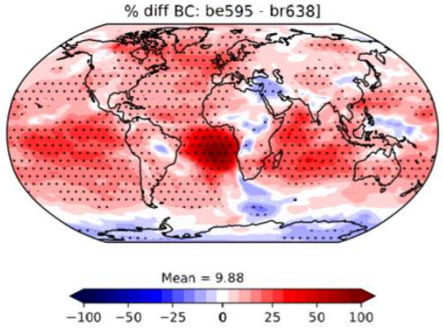

- BC mass at 600mb is increased almost everywhere
- Biggest absolute and relative increase are Tropical – SE Atlantic
- Strong relative increases over remote oceanic regions
- Some reductions over central Africa, middle East, and Antarctic.
- Relative increases at 300mb were much more uniformly spread (not shown)

Increases of BC and OC in the upper troposphere & stratosphere

BC mass concentration (ug/m^3)

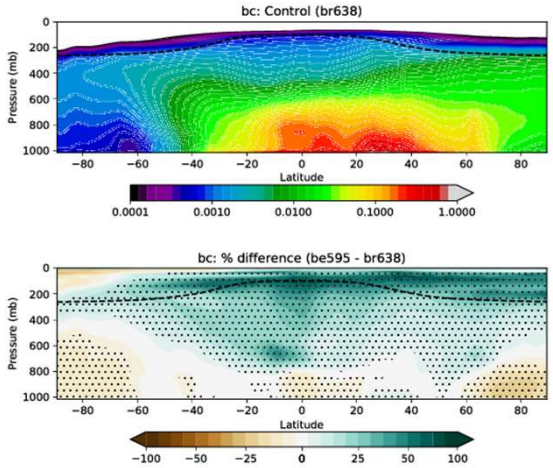

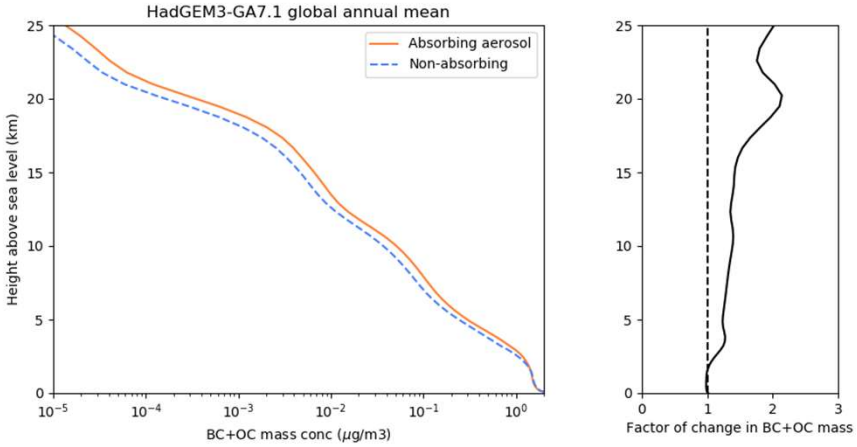

Note the logarithmic scale →

- Concentrations generally increase above 800mb
- Large relative increases in the stratosphere

- Absolute concentrations are lower higher up but large relative increases in UTLS could be important for ice-phase microphysics and heterogeneous chemistry

Does absorption increase BC mass loading?

BC column-integrated mass loading (mg/m^2)

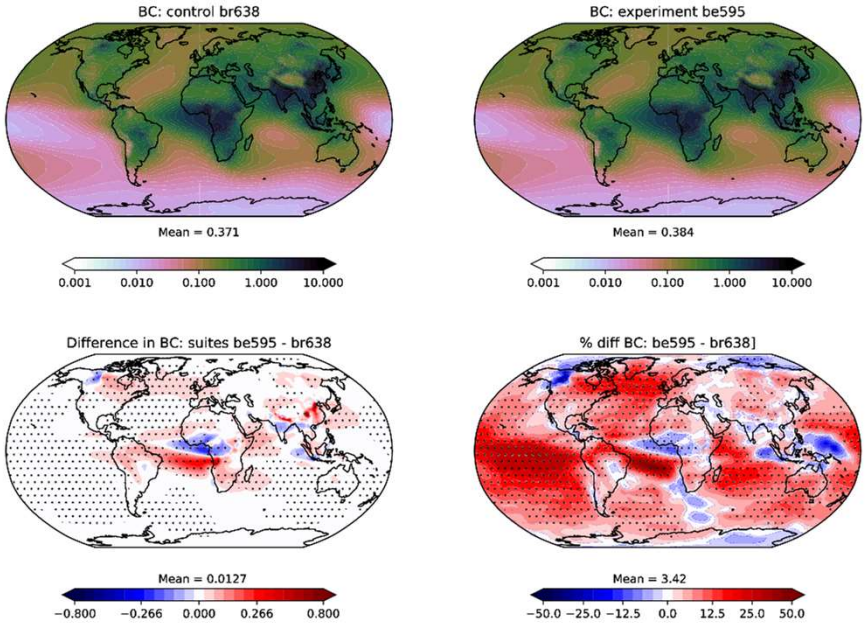

- Column mass up by 4%
- North-South shift from West Africa to Tropical Atlantic
- Strongest relative increases over remote oceans

© Crown Copyright 2020, Met Office

Elevation of aerosol layers due to SW heating

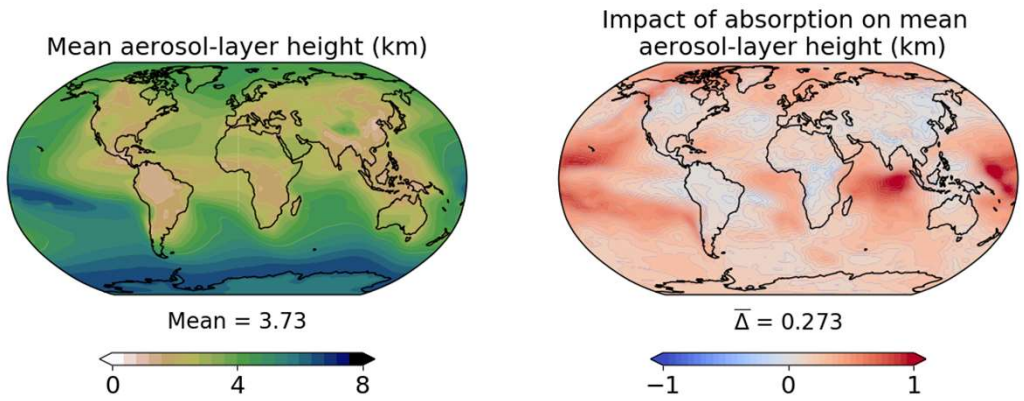

- Absorption by BC helps to raise carbonaceous aerosol (BC + OC) out of the BL into the free-troposphere (>2km)
- Carbonaceous aerosol layers rise by on average ~270m
- Biggest gains occur in remote oceanic regions affected by long-range transport of elevated aerosol layers
- Aerosol may continues to rise with time the further it is transported

Elevation of biomass burning aerosol over SE Atlantic

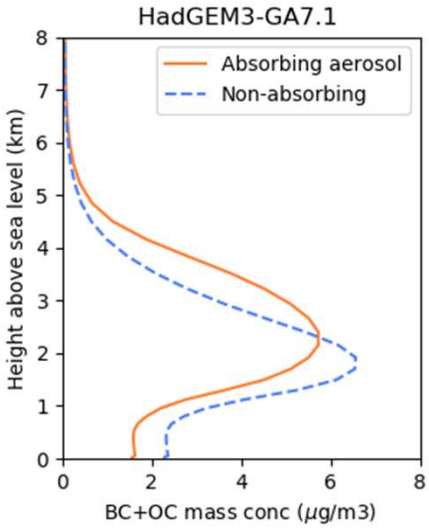

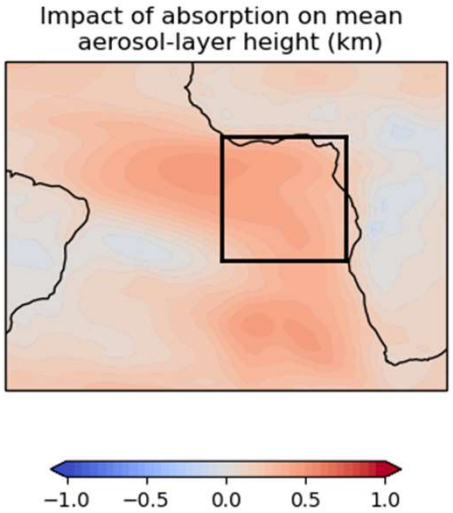

- Results are for Aug-Sept when biomass burning emissions peak
- BC heating elevates the biomass burning aerosol ~1km
- This will delay or prevent the mixing of aerosol into the stratocumulus clouds of the marine BL.
- Potentially important consequences for aerosol-cloud and aerosol-radiation interactions in this region!

Cross section of BC mass over Arctic during JJA

With absorption included:

- More BC ascends into the FT and slides up the polar front.
- Elevated layers are higher over Arctic and less makes it into the Arctic at low levels.

Control run

Absolute difference

Relative difference

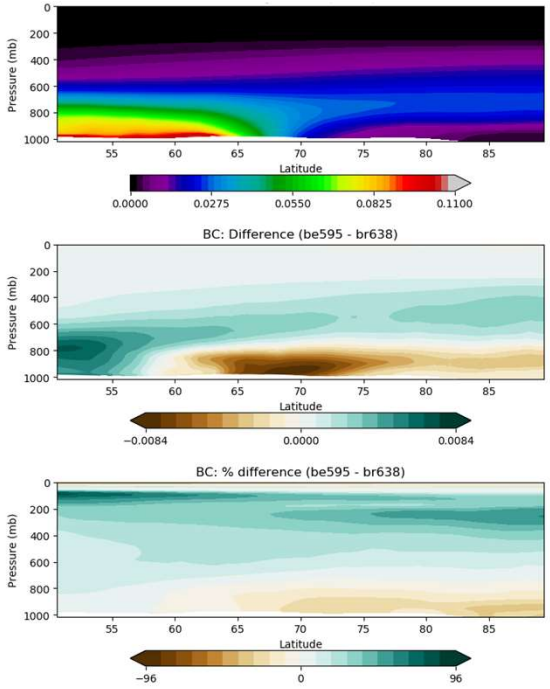

Surface BC concentration during JJA

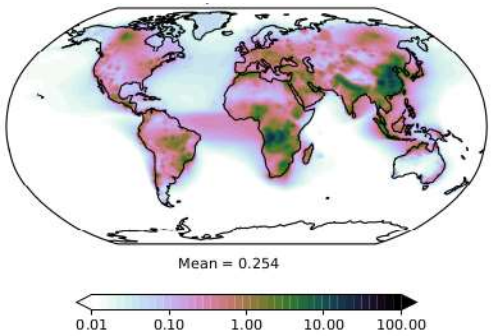

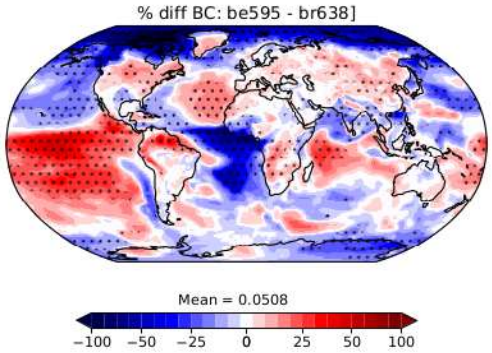

- Decreases in Arctic due to more lofting of mid-latitude sources
- Decreases over tropical-south Atlantic due to elevation of BB layer
- More surface BC over NH subtropical Atlantic and tropical-southern Pacific and Indian Ocean, presumably due to compensating descent and/or longer range transport into those regions.

Met Office
Hadley Centre

Conclusions

- Accurate representation of BC absorption / radiative heating is important for the elevation and long-range transport of the BC and other co-emitted aerosols
- Biases in the vertical distribution of biomass burning have often attributed to models failing to lift smoke at its source (plume rise), but errors in aerosol absorption properties could be just as important.
- This is potentially important for capturing the overlap between aerosol and cloud and subsequent aerosol-cloud interactions / aerosol forcing

Met Office
Hadley Centre

Single slide summary…

Self raising aerosols

BC radiative heating (700mb)

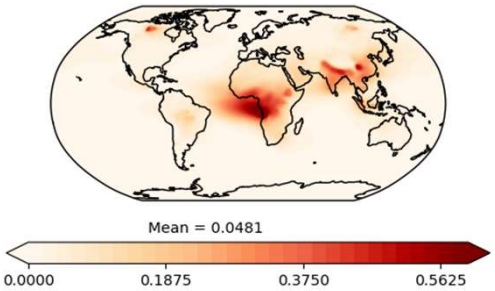

ΔW at 700mb

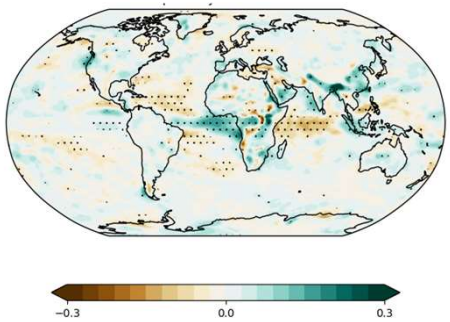

ΔBC mass (600mb)

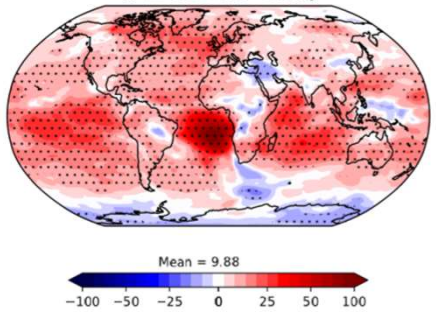

BC heating enhances uplift raising aerosol concentration in the mid troposphere and above.

Results from HadGEM3-GA7.1 experiments with BC absorption ON/OFF. Results are annual mean differences from 20 year runs.

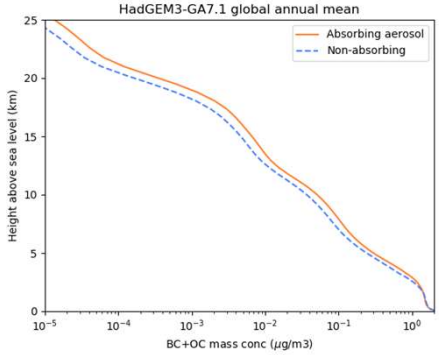

BC mass concentration (ug/m^3)

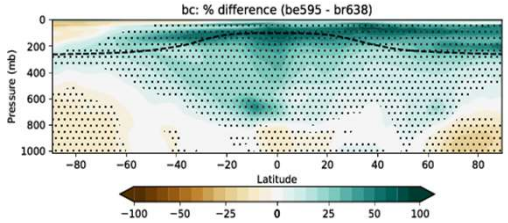

Aerosol properties from Airborne Hyper Angular Rainbow Polarimeter (AirHARP) observations during ACEPOL 2017

Anin Puthukkudy[1,2,3], J. Vanderlei Martins[1,2,3], Lorraine A. Remer[2,3], Xiaoguang Xu[2,3], Oleg Dubovik[4], Pavel Litvinov[5], and Milagros Herrera[4]

[1] Physics Department, University of Maryland Baltimore County, Baltimore, 21250, USA,
[2] Joint Center for Earth Systems Technology, University of Maryland Baltimore County, 5523 Research Park DR, Baltimore, MD 21228, USA)
[3] Earth and Space Institute, University of Maryland Baltimore County, MD, USA
[4] Laboratoire d'Optique Atmosphérique, CNRS/Université Lille, Villeneuve d'Ascq, France
[5] GRASP-SAS, Villeneuve d'Ascq, France

UMBC ESI EARTH AND SPACE INSTITUTE

UMBC NASA-GSFC JCET The Joint Center for Earth Systems Technology

LACO Laboratory for Aerosol and Cloud Optics

GRASP In principle, yes!

NASA

Automated retrieval scheme

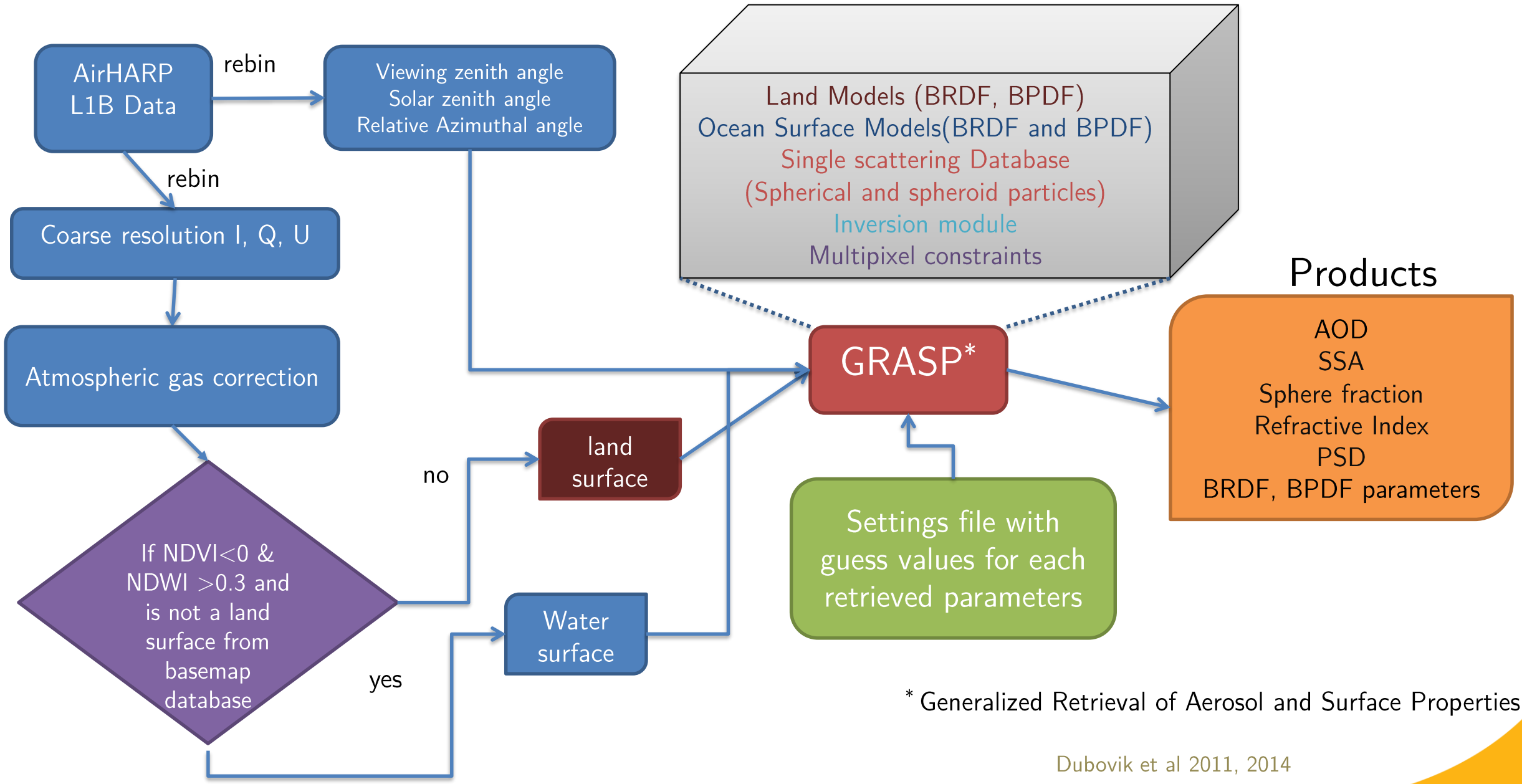

* Generalized Retrieval of Aerosol and Surface Properties

Dubovik et al 2011, 2014

Smoke case – 27 Oct 2017T18:16

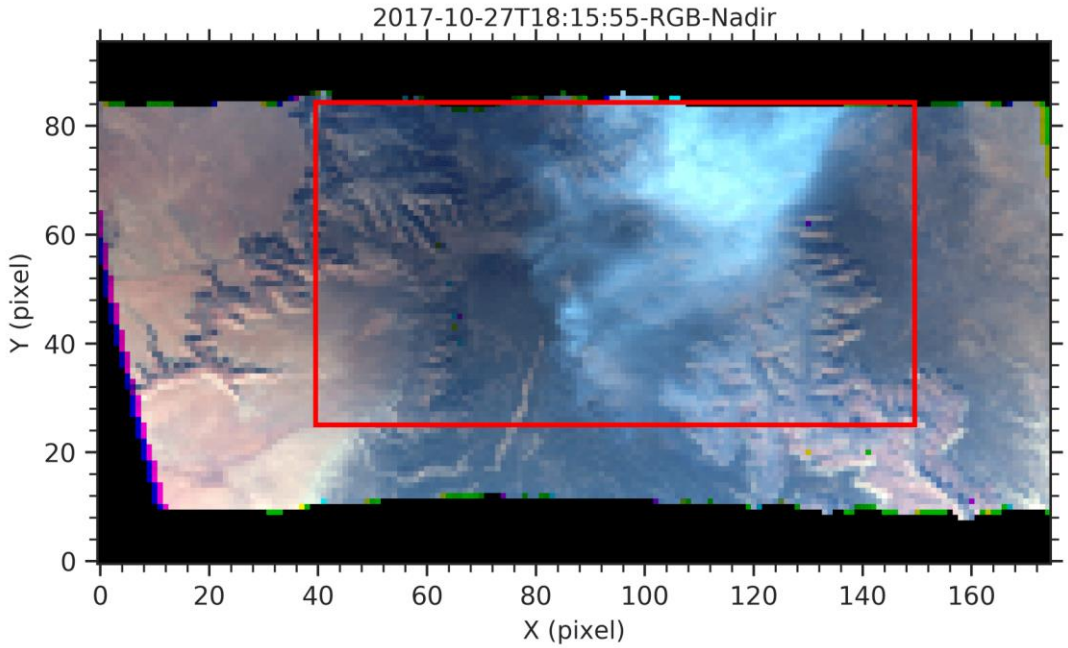

RGB image of the forest fire smoke scene near Grand canyon, AZ on 27th Oct 2017

Aerosol optical and microphysical properties retrieved for the smoke scene

Spectral band	Single scattering albedo	Spherical fraction (%)	Angstrom exponent[a]	Real refractive index (RRI)	Imaginary refractive index (RRI)
440 nm	0.87 ± 0.06	$49.9 \pm 36\,\%$[b]	1.53 ± 0.336	1.55 ± 0.04	0.024 ± 0.017
550 nm	0.86 ± 0.07				
670 nm	0.84 ± 0.08				
870 nm	0.81 ± 0.09				

[a] Angstrom exponent calculated using the AOD at wavelength bands 440 and 870 nm of the AirHARP.
[b] Retrieved spherical fraction includes a significant number of pixels with SF ~ 99 %.

Puthukkudy et al., 2020 AMT

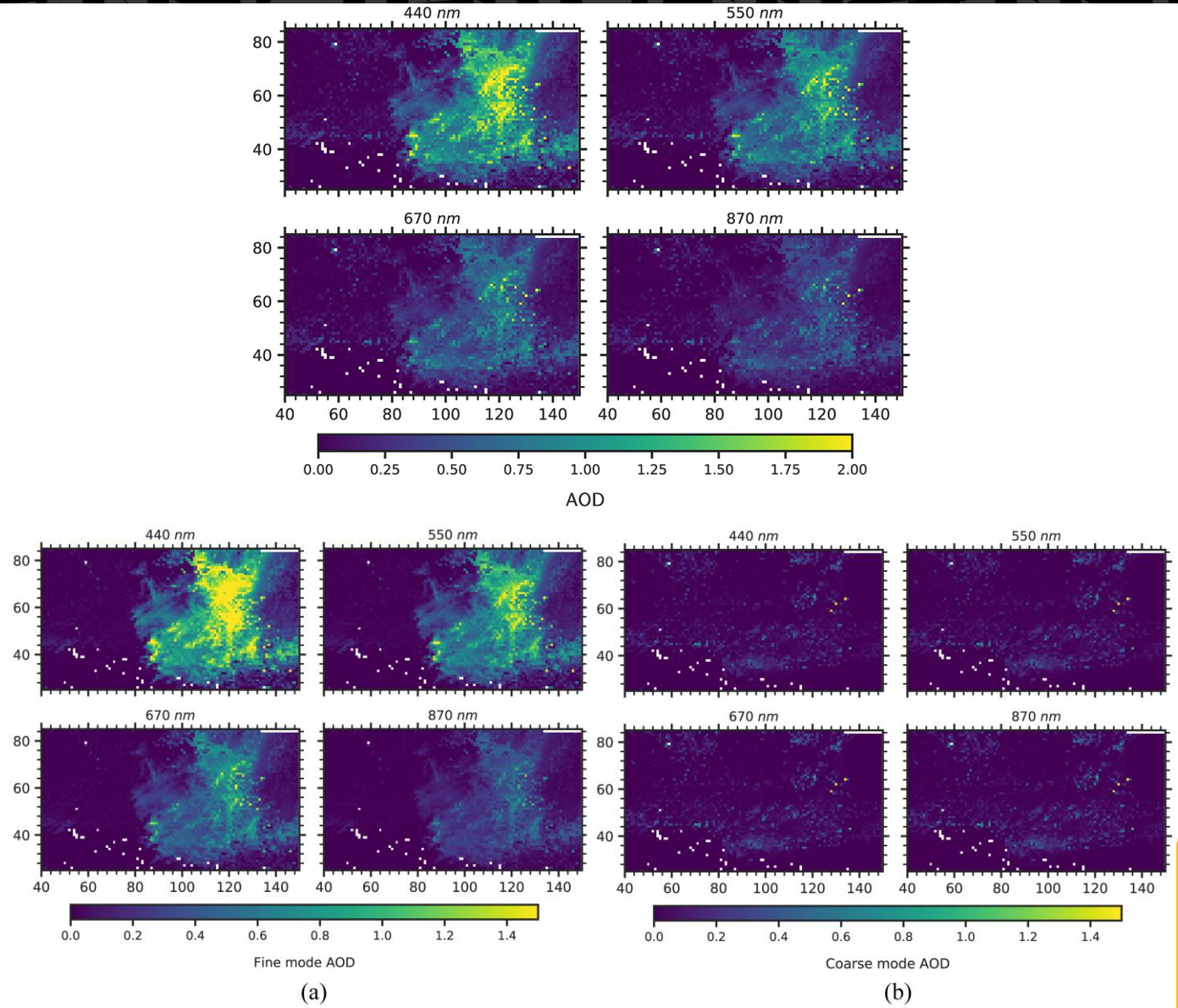

(a)Fine and (b)Coarse mode AOD retrieved using I and DoLP measurements of AirHARP at different wavelengths

Smoke case – 27 Oct 2017T18:16

Aerosol Optical Depth

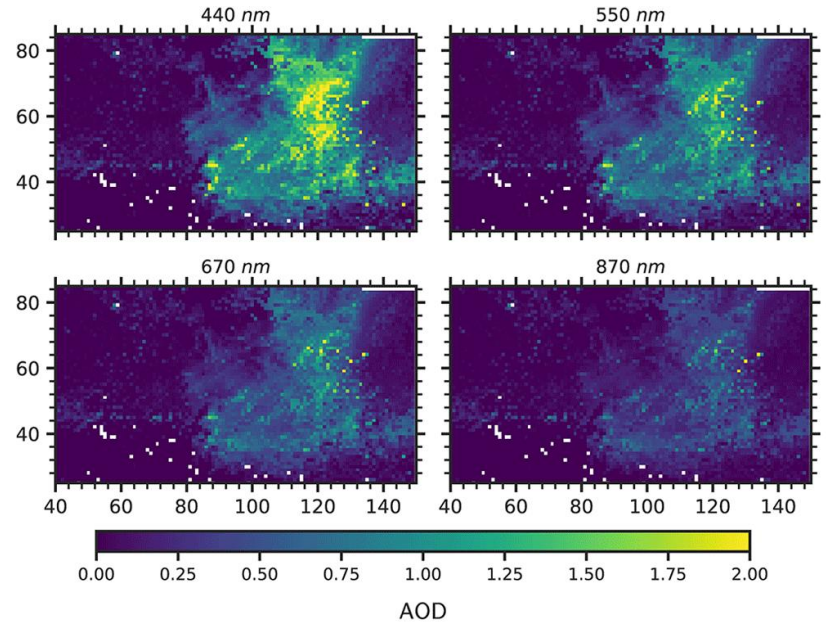

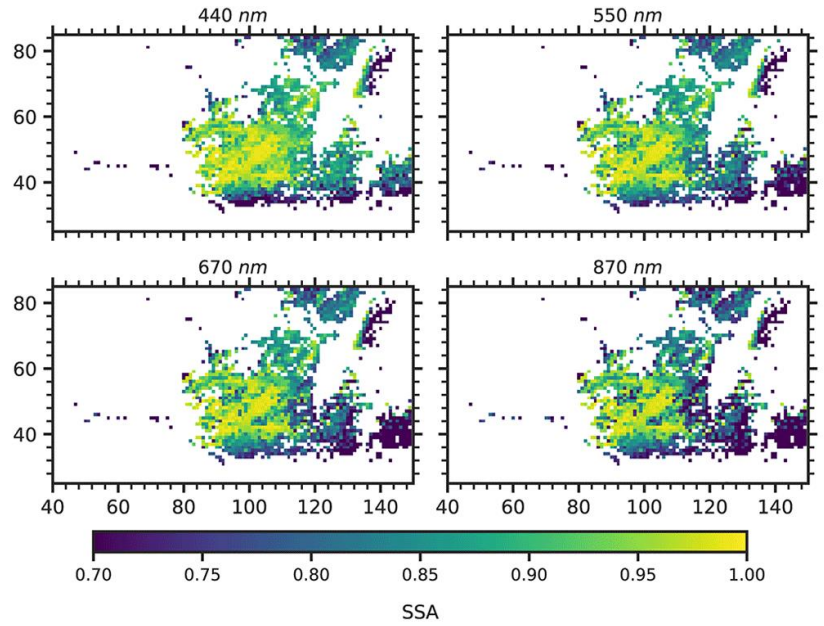

Single Scattering Albedo

Real Refractive Index

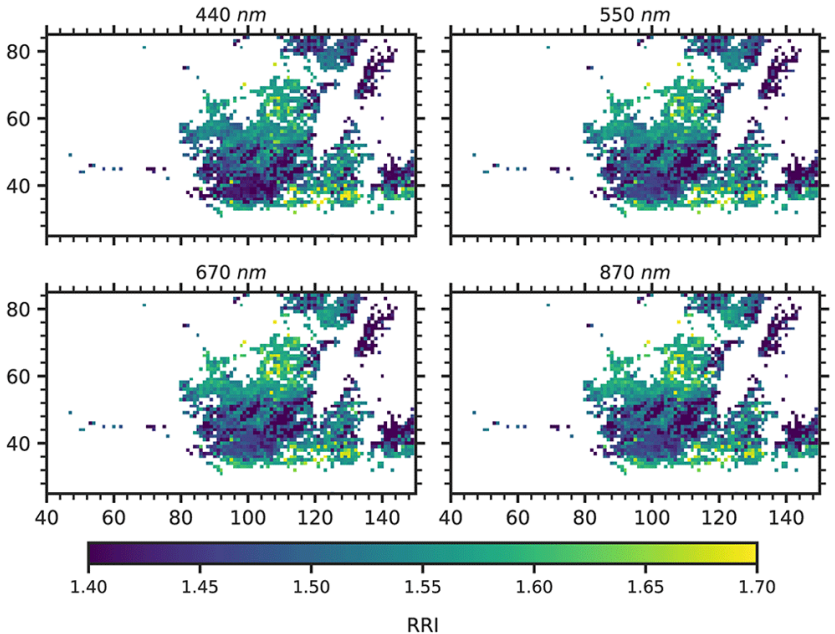

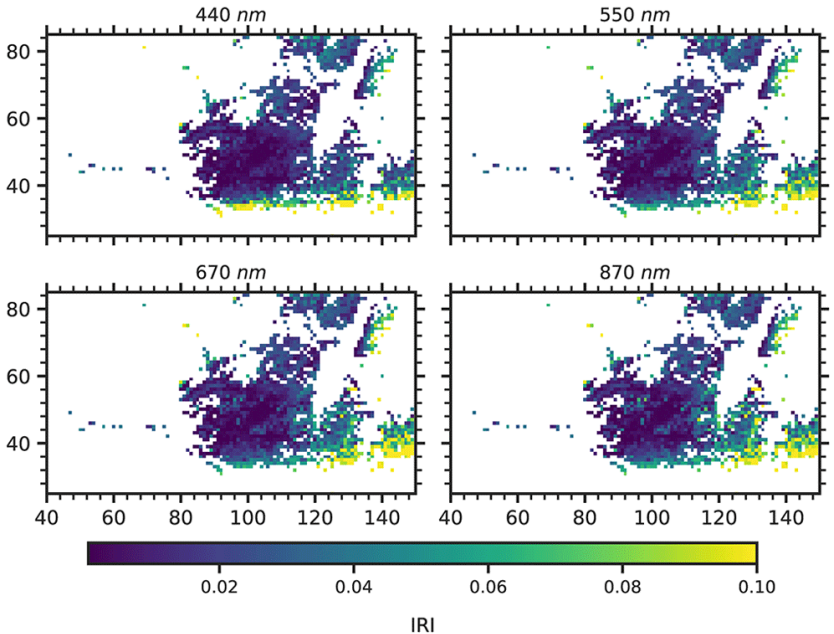

Imaginary Refractive Index

AERONET AOD Comparison

GRASP/Five mode kernel:Five log-normal modes used for particle size distribution in GRASP retrieval for AirHARP; r_v is the volume median radius and $\log(\sigma_v)$ the geometric standard deviation (SD). In this kernel, other particle properties are free to be retrieved

r_v (μm)	$\log(\sigma_v)$
0.1	0.35
0.1732	0.35
0.3	0.35
1.0	0.5
2.9	0.5

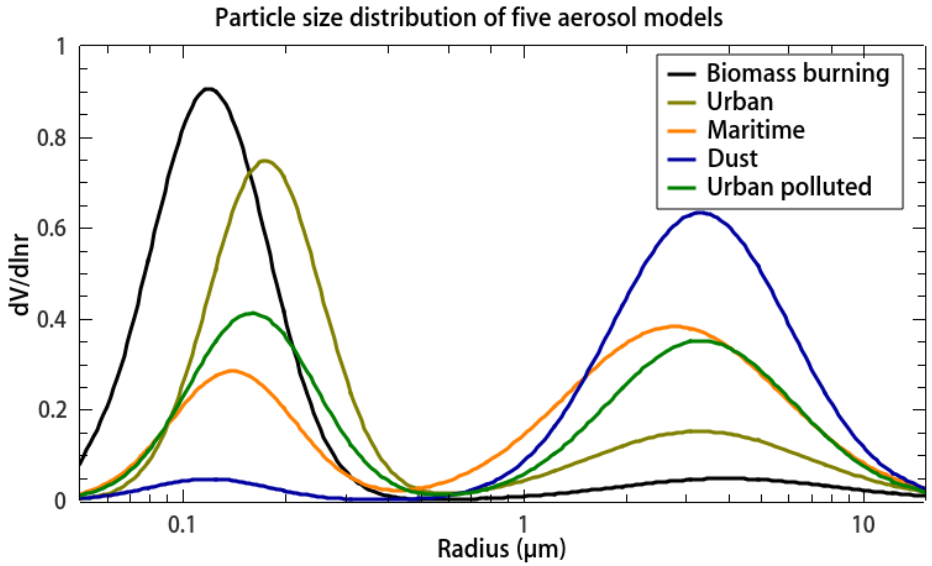

PSD of the aerosol components used in the GRASP/Models kernel

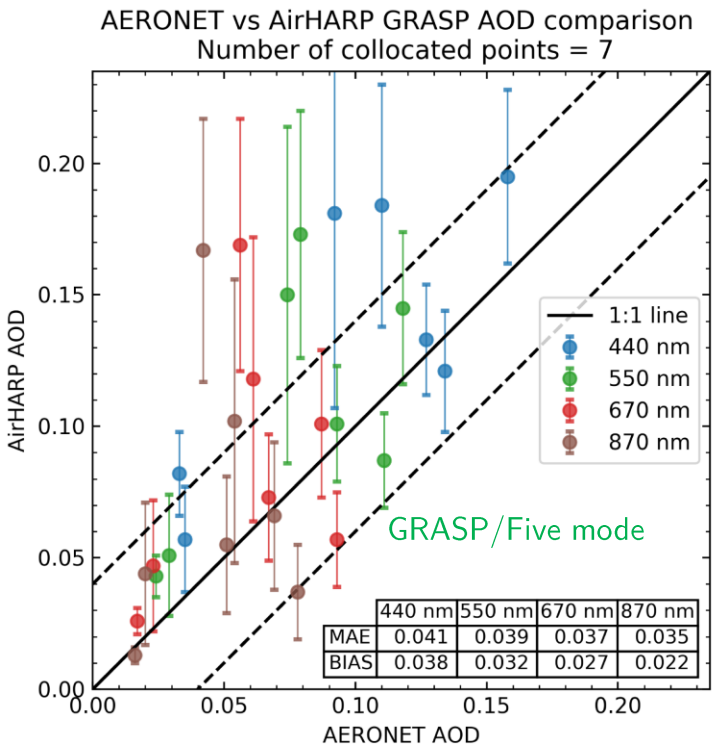

(a)

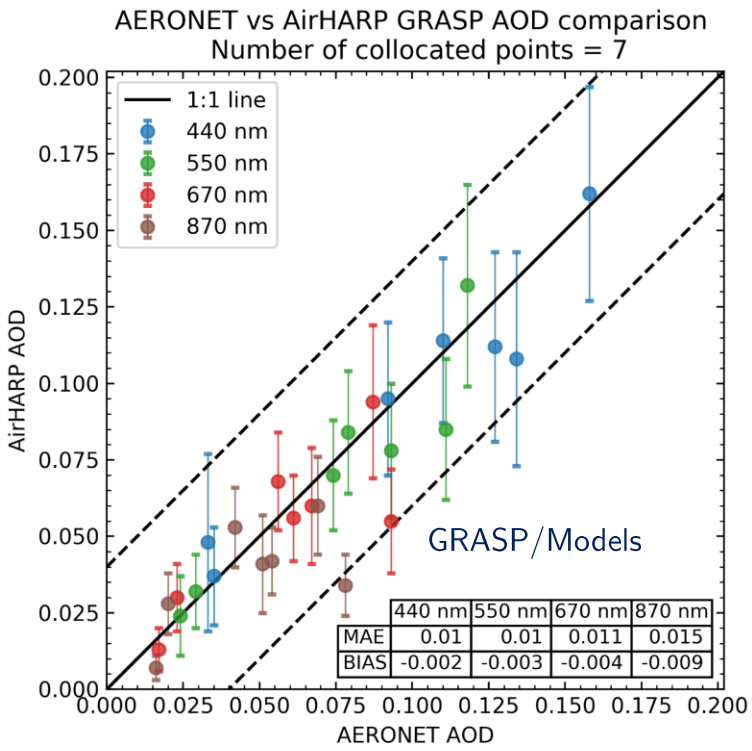

(b)

Scatter plot of AERONET AOD vs AirHARP GRASP AOD retrieved. Pixels with a resolution of 550m x550m are used for the retrievals. Each circle in the figure is the mean of 10x10 pixels(5.5km x 5.5km) around the respective AERONET station. (a) using GRASP/Five mode kernel and (b) using GRASP/Models kernel

HSRL2 comparison

(a)

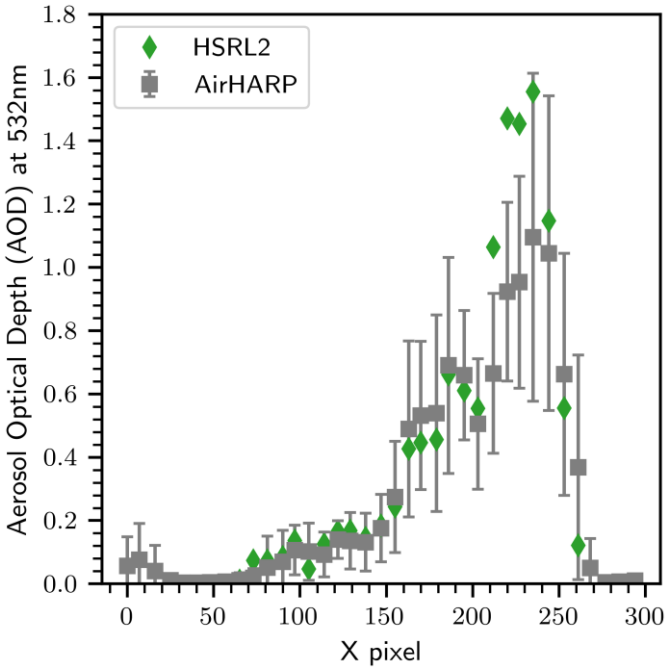

(b)

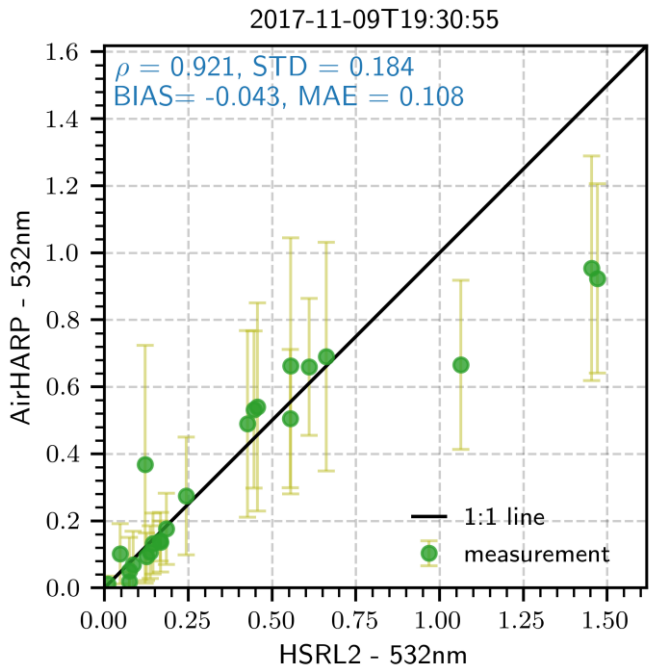

(a) AOD measured at 532nm by AirHARP versus HSRL2 AOD at 532nm for the forest fire scene on 09-11-17_07,31,00PM ; (b) Correlation plot for the HSRL2 AOD at 532nm vs AirHARP AOD at 532nm for the flight on 9th November 2017 over a smoke plume. (c) Comparison of Angstrom Exponent from HSRL2 measurement and AirHARP-GRASP retrievals

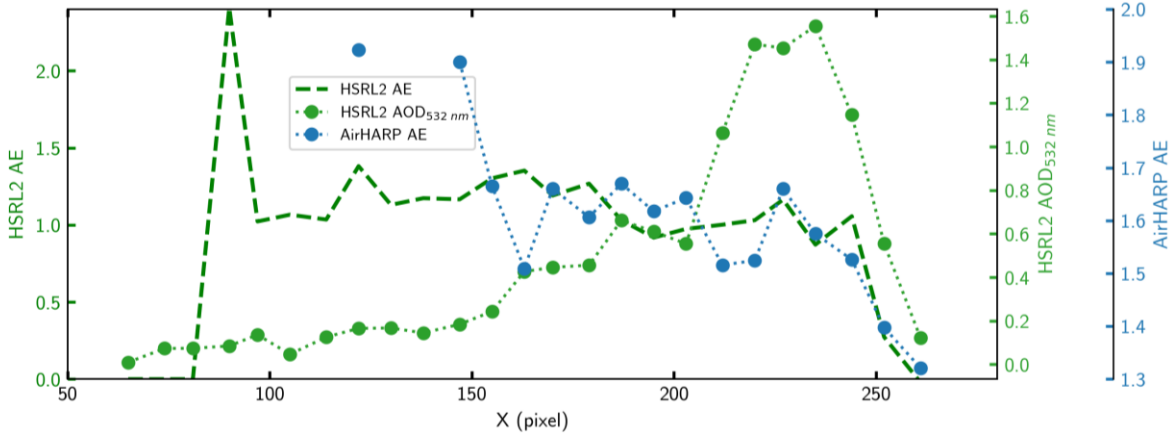

Comparison of HSRL2 Angstrom exponent (AE) (355 and 532 nm) with AirHARP retrieved AE (440 and 870 nm)

(a)

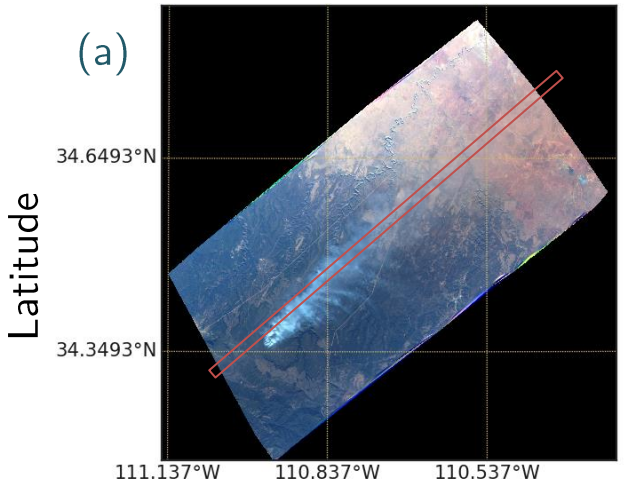

(b)

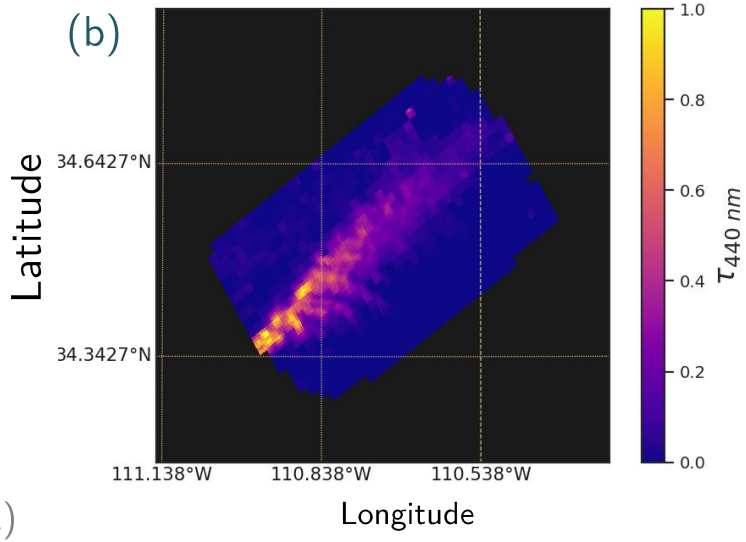

(a) Projected RGB image and (b) $AOD_{440\ nm}$ map from AirHARP GRASP retrievals for the scene on 09-November-2017 T19:30:55 UTC

Breakout session 4

- Suborbital measurements and biomass burning
  - Ferrare, Richard: Biomass Burning over the SE Atlantic
  - Eck, Thomas: AERONET ext. wavelength retrievals of absorption
  - Hahn, Valerian: Increased reflectance by polluted low-level clouds
  - Puthukkudy, Anin: Aerosol properties from the AirHARP Polarimeter
  - Johnson, Ben: Self-raising aerosol
- Plenary Session 6 – COVID-19 impact on aerosol load, air quality, and forcing.
  - Bellouin, Nicolas: Impact of Chinese Covid-19 lockdown
  - Kondragunta, Shobha: China and Taiwan: 2 diff COVID-19 lockdowns
  - Liu, Xiaohong: Impacts of COVID-19 on rad. forcing
  - Quaas, Johannes: Aviation-induced cirrus during COVID-19
  - Skeie, Ragnhild: Aerosol and rad. forcing due to COVID-19
  - Tsyro, Svetlana: Impacts of COVID-19 lockdown on EU air quality
  - Mortier, Augustin: COVID-19: Impact on AOD and EU Air Quality